

Smart real-time scheduling of generating units in an electricity market considering environmental aspects and physical constraints of generators



Arman Goudarzi^a, Andrew G. Swanson^a, John Van Coller^b, Pierluigi Siano^{c,*}

^a School of Electrical, Electronic and Computer Engineering, University of KwaZulu-Natal, South Africa

^b School of Electrical and Information Engineering, University of the Witwatersrand, South Africa

^c Department of Industrial Engineering, University of Salerno, Fisciano, Italy

HIGHLIGHTS

- Considering several physical and environmental constraints of generating units.
- Proposing a hybrid method based on LSSVM-CA3 for solving the CEED problem.
- Real-time scheduling of generating units in electricity spot markets.
- A holistic optimization method for real-time prediction in a dynamic environment.

ARTICLE INFO

Article history:

Received 6 August 2016

Received in revised form 17 November 2016

Accepted 12 December 2016

Keywords:

Combined environmental economic dispatch

The third version of the cultural algorithm (CA3)

Least square support vector machine (LSSVM)

Real-time scheduling

Physical constraints of generators

ABSTRACT

Optimal scheduling of generating resources plays a significant role as a decision-making tool for power system operators in the liberalized and real-time electricity spot markets. The real-time scheduling of generating units will become a very complex task with respect to the instantaneous fluctuation of the load demand due to several demand response scenarios in the smart grid context. In this study, a hybrid mathematical method for the online scheduling of units based on the least square support vector machine (LSSVM) and the third version of cultural algorithm (CA3) has been presented, where the CA3 has been specifically employed to tune the adjusting parameters of LSSVM. For the training purpose of the proposed method, the optimal scheduling of the daily load curve for four different test systems and various physical and environmental constraints of generating units have been prepared by using a modified mixed integer quadratic programming (MIQP) to deal with non-convex behaviors of the test systems. A mean squared error (MSE) objective function has been used to reduce the prediction errors during the training process to enhance the precision and reliability of the results. A radial basis function (RBF) and the proposed LSSVM-CA3 were used to check the convergence process. A high accuracy of generator schedule predictions are demonstrated by comparing the results of the proposed method with those of artificial neural networks. From the results, it can be inferred that the method is highly compatible for real-time dispatching of generation resources in deregulated electricity markets.

© 2016 Elsevier Ltd. All rights reserved.

1. Introduction

Due to deregulation of power systems, it is vital to operate the power grid with the highest possible degree of reliability and economy to enhance the competition of power plants in liberalized electricity markets. This problem can be solved by the economic

load dispatch (ELD) problem through a set of sophisticated computational skills which tackle different power grid constraints [1]. The aim of the ELD problem is to define the optimal scheduling of generating units which minimizes the total generation cost while all the operational constraints and the load demand are satisfied. This task can be very challenging when considering the environmental aspects of conventional generators, such as coal, oil and natural gas units. The reduction of fossil-fuel based generation resources and the improvement of their energy efficiency is a foremost priority of the energy roadmaps in many countries worldwide [2]. In

* Corresponding author.

E-mail addresses: goudarzia@ukzn.ac.za (A. Goudarzi), swanson@ukzn.ac.za (A. G. Swanson), john.vancoller@wits.ac.za (J. Van Coller), psiano@unisa.it (P. Siano).

Nomenclature

Indexes

ANN	artificial neural network
CA3	third version of the cultural algorithm
CEED	combined environmental economic dispatch
CF	cost function
KKT	Karush-Kuhn-Tucker
LSSVM	least square support vector machine
MSE	mean squared error
MAE	mean absolute error
NRMSE	normalized root mean squared error
RBF	radial basis function
RMSE	root mean squared error
PF	penalization factor
PPF	price penalty factor
POZ	prohibited operating zone
SVM	support vector machine

Variables

a_i, b_i, c_i	fuel cost coefficients of unit i
$\alpha_i, \beta_i, \gamma_i, \eta_i, \delta_i$	emission cost coefficients of unit i
d_i, e_i	fuel cost coefficients of unit i regarding valve-point effects
$B(t)$	belief space of cultural algorithm
$F_{ct}(P_i^t)$	total CEED generation cost at time t
$f_{emc}(P_i^t)$	emission cost function at time t
$f_{gc}(P_i^t)$	generation cost function at time t
$h_i^{max-max}$	max-max price penalty factor
$I_j(t)$	closed interval of $N(t)$
l, u	the lower and upper bound which are initialized by the domain values
$L_j(t)$	score of the lower bound at $N(t)$
N_G	number of generating units
$N(t)$	normative knowledge component of the cultural algorithm

N_{ij}	a normalized number for individual i and component j
n_s	number of variables of the situational component
n_x	number of variables of the normative component
nz_i	number of prohibited zones for unit i
ψ	sets of units with POZ
Ψ	sets of units with S_R
P_i^t	power output of unit i at time t
P_D^t	load demand of the system at time t
P_i^0	previous output power ($t - 1$)
$P_{i,1}^t$	lower bound of unit i at the first prohibited zone i
P_i^{min}, P_i^{max}	minimum and maximum generation limits of the i th generating unit
$P_{i,m}^t, P_{i,m-1}^U$	lower and upper bound of the m th prohibited zones of unit i
$P_{i,N_i^{pz}}^U$	the last upper bound of the nz th prohibited zones of unit i
$S(t)$	situational knowledge component of the cultural algorithm
S_i^t	spinning reserve from unit i at time t
S_R	total system spinning reserve requirement
S_i^{max}	maximum spinning reserve contribution of unit i
δ_j	step size of the belief interval
$\delta_j^2(t)$	the variance of normalized number N_{ij}
$U_j(t)$	score of the upper bound of $N(t)$
UR_i, DR_i	up and down ramp rate limits of unit i
$X_j(t)$	dimension of belief space at component j
$X_i(t)$	an accepted response
$x_{ij}(t)$	the mean of normalized number N_{ij}
$x_{lj}(t)$	an accepted response of the component j
$\hat{x}_{ij}(t)$	influence function
$x_j^{min}(t), x_j^{max}(t)$	minimum and maximum boundary of the closed interval at generation t
$\hat{y}(t)$	best individual of the solution vector

addition, conventional generators may have physical constraints, such as prohibited operating zones (POZs) which is associated with their steam valve operation or any vibration in their shaft bearings. The operating area of generating units that have POZs can be divided into a number of feasible sub-regions. This issue converts the classical ELD problem into a non-convex and nonlinear problem with discontinuous operating zones, where the problem simultaneously requires the minimization of the total generation cost and the emission level while maintaining the equality and inequality constraints of the system [3]. The new resulting problem is called combined environmental economic dispatch (CEED). Classical approaches, such as the gradient method, linear programming, the lambda iteration method, quadratic programming, the base point and participation factors method, and the Lagrange relaxation algorithm, have substantial difficulty in dealing with the CEED problem [4]. New types of deterministic optimization algorithms with the inclusion of modification techniques such as mixed integer programming, nonlinear programming algorithm and dynamic programming for solving the CEED problem have been presented [5]. As the CEED problem is the main subroutine of a bigger problem, the so-called unit commitment (UC), and lots of valuable contributions with respect to deterministic optimization algorithms have been made in this area. Therefore, it would be appreciated to tackle some of the recent innovative solutions for the UC and its applications. Koltsaklis et al. [6] presented a

generic mixed-integer linear programming (MILP) which incorporates a unit commitment solution for daily energy planning with a long-term generation expansion framework with several system considerations including ramping limits, system reserve requirements, renewable penetration limits as well as the CO₂ emission effects of conventional generation resources. The same authors developed a mid-term energy planning (MEP) model through a unit commitment model for generation and transmission system planning with an ability to perform a day-ahead electricity market calculation for yearly basis. Their proposed method is capable of quantifying the effects of different costs on the day-ahead electricity market and the energy mixture of the system [7].

Niknam et al. [8] proposed a new mathematical solution for the UC problem based on benders decomposition where the solution divides the UC into a master problem and a sub-problem. They have tried to solve the master problem with help of the mixed integer optimization where a non-linear optimization has been assigned to take care of the sub-problem. Simoglou et al. [9] presented a new 0/1 MILP formulation for the self-scheduling of thermal generation resources in the co-optimized energy and reserve day-ahead markets where the generating units start-up cost has been divided into three subcategories as hot, warm and cold through to each predefined power output trajectories. Delarue et al. [10] investigated the effect of uncertainty of the load and wind generation on the multi-day ahead UC where they have

assumed the perfect prediction of the load demand for initial hours as the starting point. Thereafter, the consecutive UCs have been performed to find the optimal scheduling of the generating units where the new load forecasts have been achieved through different percentages of the load deviation and a number of test system scenarios. A novel UC-MILP based on branch and bound method is modeled in [11], where they have proposed three sets of symmetry breaking constraints for UC according to different considered time horizons.

Some of the recent studies in the area of the UC have attempted to model the intermittent behavior of wind energy in order to investigate the influence of wind power output on the scheduling of the other thermal units. Wang et al. [12] analyzed the impacts of the high level of wind penetration on thermal generation with a stochastic UC model while they have used a point forecast method to capture the uncertainty of the wind power output. In [13] a new model of UC based on a modified bender decomposition has been presented, where the developed model has the ability to capture the sub-hourly variability of the wind power. Most of the deterministic optimization algorithms have difficulty in finding the optimal solution for large-scale power systems with mixed generation resources, where these methods fall into local minima due to the oscillation of their decision parameters resulting in an increase in the computation time.

In the past few decades, many evolutionary computational algorithms such as genetic algorithm (GA) [14], particle swarm optimization (PSO) [15], artificial bee colony (ABC) [16], harmony search (HS) [17] and tabu search algorithm (TSA) [18] have been used to solve power system problems. Most of the probabilistic or metaheuristic algorithms are inspired by nature through global search space properties. Secui aimed at solving dynamic economic dispatch through a modified ant colony optimization algorithm by considering the valve-point effect on the generation cost [19]. A combination of a chaotic self-adaptive and a differential harmony search algorithm has been proposed to find the optimal scheduling of generating units in [20]. Xiong et al. [21] proposed a multi-strategy ensemble biogeography-based optimization (MseBBO) for solving the ELD problem, where they have added three extensions to the main components of the BBO (migration model, migration operator and mutation operator). Their proposed method simultaneously makes a balance between exploration and exploitation in the search space in order to enhance the efficiency of the optimization process. Alsumait et al. [22] presented a new hybrid intelligent approach based on GA, pattern search (PS) and sequential quadratic programming (SQP) to solve the ELD problem while considering the valve-point effect, where each one of the optimizers has been assigned a separate task. In the same study, GA has been assigned as the main optimizer, whereas PS and SQP are utilized to adjust different tuning parameters of GA to increase the accuracy of the solution. Tsai et al. [23] developed a new PSO algorithm with a constriction factor (PSO-CF) for the trading of CO₂ emission cost embedded into traditional ELD. They have introduced two operators, called random particles, and fine-tuning to improve the drawbacks of the classical PSO in searching for the global optimum. In [24], the authors proposed an environmental-economic dispatch model which simultaneously considers carbon capture plant scheme and uncertainty of wind generation in the framework of a two-stage robust optimization. Since both objectives are convex functions, they have utilized the Pareto front in combination with the ϵ -constraint method to find the optimal scheduling of generating units. The Nash bargaining criterion has been used to determine the fair trade-off between the generation cost and the carbon emission. In [25], a hybrid evolutionary algorithm for solving the ELD problem with the consideration of the valve-point effect has been formulated. The presented method combines a fuzzy adaptive PSO with the Nelder-Mean (NM) search method

called (FAPSO-NM). In order to enhance the effectiveness of their algorithm, the NM algorithm has been assigned as a local search algorithm in surrounding of the global solution found by FAPSO. In [26], a hybrid method for solving dynamic economic emission dispatch based on chemical reduction optimization (CRO) has been presented, while for the reduction of the computational time a differential evolution algorithm has been incorporated with CRO. In [27], the CEED problem has been solved through the PSO method, while two important factors of the power market such as transmission congestion distribution (TCD) and reactive TCD have been taken into account. The usage of metaheuristic optimization algorithms to solve real world problems has gained the interest of numerous researchers around the globe due to their efficiency. However, most of these methods require to be executed several times to find the best solution, therefore they are not time efficient for real-time electricity market operation with the large-scale of generating units connected to the power grid.

In the last few years, another type of metaheuristic algorithm and artificial intelligence which is based on the concept of the human brain process has been employed to solve the CEED problem. The artificial neural networks (ANNs) have the ability to learn the behavior of the power grid through the online observation of the system or through historical data. The ANNs are then able to predict the possible solutions for the objective function. An enhanced augmented Lagrange Hopfield neural network (ALHN) is presented in [28] and used to solve the economic dispatch while the cost function has been considered as a piecewise quadratic cost. Their proposed method investigated the problem in two phases; in the first phase, a heuristic optimization method was used to select the type of fuel for each generating unit of the system and in the second phase the ALHN was used to find the optimal solution of the economic dispatch with respect to the chosen fuel type. Canizes and his colleagues proposed a method to determine the required reserve level for the electricity market dispatching system [29]. Their proposed method was based on submitting bids from the generators to the spot market where the market clearing prices were calculated by a mixed integer non-linear programming algorithm. After the collection of the market prices and generator schedules, an ANN was used to predict the required level of spinning and non-spinning reserve for a day-ahead market. In [30], a robust radial basis kernel function (RBFK) based on an ANN was developed to solve the CEED problem, where the max-price penalty factor was used to convert the emission volume into its respective price. In [31], a methodology using a combination of orthogonal least-squares (OLS) and enhanced particle swarm optimization (EPSO) algorithms to build a three layers RBF network for real-time CEED has been proposed. Kar et al. used a hybrid ANN based on the back-propagation algorithm (BP-ANN) to find the optimum solution of the CEED problem where the volume of NO_x was optimally regulated [32]. The adjusting parameters of the BP algorithm were optimally tuned during the convergence process, while the influence of other types of normalization rules and adjusting parameters, such as the number of hidden layers, the number of nodes in the hidden layers have been considered in [32].

Almost all the different types of neural networks based methods have some deficiencies in defining the network structure, and this problem would specifically increase the running time for real-time applications of ANN methods in a dynamic environment [33]. In addition, ANNs have a large number of adjusting parameters including the number of hidden layers, the number of neurons, input weight matrices, layer weight matrices and bias vectors, etc., and it requires the human interferences during the optimization process. In contrast to ANNs, support vector machines (SVMs) have an uncomplicated structure with only two adjusting parameters (which significantly reduces the running time of prediction

process) as well as having the capability to be applied to any function within a dynamic environment. The basic concept of SVMs is based on the machine learning pattern, which was initially developed to solve classification problems [34]. SVMs present a promising performance in linear and non-linear identification applications through the use of linear constrained quadratic programming (QP) and Vapnik's ϵ -insensitive loss function, respectively. In [35], a hybrid method based on GA and SVM was proposed for the identification of electricity fraud through the daily load profile, where the SVM detected abnormalities due to a fraud incident. In order to enhance the capability of SVM, Mustafa et al., coupled the classic SVM with the least-square method as well as a variant model of artificial bee colony to forecast the crude oil prices based on the time series data [36]. In [37], a method based on LSSVM and independent component analysis (ICA) optimizer has been presented for short term load forecasting. In order to enhance the prediction accuracy of LSSVM, the ICA transformed the dimensions of the input data from a higher level into a lower level, which also decreased the complexity of the model structure for the LSSVM.

The main idea of this study is to propose a methodology to calculate the optimal dispatch of generating units in the real-time electricity market, where the generator schedules must be evaluated in less than 15 min. The proposed method has the capability to predict the optimal dispatches of generating units with the high level of accuracy in less than 10 s for a large-scale power system, where it is approximately 100 times faster than the other widely industrial used methods such as MIQP considering the physical and environmental constraints of generators. In order to understand the behavior of any system in a suitable manner, the proposed method (LSSVM-CA3) requires historical data based on the hourly load curve of the system for at least one day. Thereafter, it has the ability to predict any unknown load point within the daily load curve with a high level of precision. In this regard, the following sophisticated mathematical formulation has been proposed.

The third version of cultural algorithm (CA3) has recently been proposed by Goudarzi et al. [38]. CA3 has demonstrated a high capability of solving non-convex problems with a high degree of non-linearity. In this study, CA3 was used to optimally tune the two adjusting parameters of the LSSVM (γ and σ^2) in order to decrease the estimated error of the objective function. In order to prepare the training data set, a modified mixed integer quadratic programming (MIQP) has been used to obtain the optimum scheduling of the generating units according to the daily load curve of the selected test systems. To investigate the practicality of the proposed method (LSSVM-CA3), it has been compared with other hybrid methods of ANNs. The main innovative contributions of the proposed method are as follows:

- i. A hybrid mathematical method for the prediction of the behavior of any dynamic system based on the least square support vector machine and the third version of the cultural algorithm (LSSVM-CA3) has been proposed.
- ii. The proposed method has the ability to understand and predict the non-linear behavior of the power grid considering several realistic physical constraints of generating units for solving the CEED problem.
- iii. The proposed method has the capability to comprehend and predict the environmental aspects of generating units in the real-time analysis of a large-scale power system.
- iv. The proposed method is capable of finding the optimum schedule of generating units for a large-scale power system in a real-time electricity market within an extremely fast calculation time.

- v. The proposed method is capable of maximization of social welfare while minimization of total cost of generation in the real-time electricity market.

The organization of the paper is as follows. Section 1 describes the background of the study through a comprehensive introduction. Section 2 demonstrates the problem formulation and mathematical concepts of the proposed method. Section 3 provides the discussion of the obtained results. The conclusion is given in Section 4.

2. Problem formulation

2.1. Time window for the wholesale electricity market operation

As the main focus of study is the real-time scheduling of generating units in the electricity market, the time frame for the market operation is depicted in Fig. 1. All the given terminologies in Fig. 1 are defined as follows:

- **Capacity Market:** This is designed to guarantee an adequate and reliable generating capacity and is always available by providing payments to encourage investment in new capacity or for existing capacity to remain open. In other words, it is the primary policy of any market operation to ensure the security of electricity supply, while it has a time span from 1 to 5 years [39].
- **Multi Day-ahead Unit Commitment:** the unit commitment schedule of the dispatchable generating units should be prepared by the system operator in less than 24 h while the physical constraints of the generating units should be considered. In this context, hydro and nuclear units would be treated as must-run units (to be responsible for the base-load) in the day-ahead market.
- **Day-ahead Market:** market participants are required to submit their bids or offer within a pre-specified submission time. The contracts will be settled between seller and buyer for the delivery of power in the following day, where the price is set and the trade is agreed. It is vital to indicate that the offers or bids are the financial key performances of any business process [40]. The detailed operations for day-ahead market can be listed as follows [41]:
 - 24 h ahead scheduling considering the load forecast of the next day
 - Determining the commitment of the slow thermal units
- **Intraday Scheduling:** the intraday scheduling supplements the day-ahead market and provides any necessary changes to balance between supply and demand. The detailed operations for intraday scheduling can be listed as follows [41]:
 - 4 h ahead scheduling of generators (until cover the entire day)
 - Determining the commitment of the fast operating units



Fig. 1. Time frame of the electricity market operation.

- **Real-time Market:** the system operator is required to provide the generating unit dispatches, reserve margins, real-time locational marginal prices (LMPs) and market clearing prices (MCPs) every 5–15 min.

2.2. Combined environmental economic dispatch (CEED)

The main elements of the electrical power grid which have a significant influence to deliver the power generation at the least cost are optimum scheduling of generating units, fuel cost, and transmission line losses. The most effective generating unit in the power grid is not able to guarantee to decrease or minimize the total generation cost as it may be located far away from the load demand which would effectively lead to greater transmission losses or a variation in the fuel cost according to the geographical location of generating units. The main aim of the combined environmental economic dispatch (CEED) method is to minimize the total generation cost by satisfying the power grid operation constraints and considering the environmental aspects of generation [42].

The generation cost function of the CEED method can be defined as follows:

$$f_{gc}(P_i^t) = \sum_{i=1}^{N_G} (a_i + b_i P_i^t + c_i (P_i^t)^2) \quad (1)$$

In the conventional approach, economic load dispatch (ELD) makes a simplification by assuming that the efficiency of the electrical power generators increases cubically, quadratically, piecewise linearly or sometimes can be formulated linearly with respect to the power output. In real life practice, the volume of the steam entering the turbines would be controlled by sets of separate nozzles. Each one of the nozzle sets accomplishes the best efficiency when the generating unit is operating at full capacity. By increasing the power output of the generating units, their respective valves will be opened in series to obtain the highest possible efficiency for the considered power output. The valve-point effect introduces a ripple in the heat rate function which leads to non-linearity and discontinuity of the fuel cost function [43]. A rectified sinusoidal term can be added to the previous equation for precise modeling of the generator cost function with the consideration of the valve-point effect.

$$f_{gc}(P_i^t) = \sum_{i=1}^{N_G} [(a_i + b_i P_i^t + c_i (P_i^t)^2) + |d_i \times \sin\{e_i \times (P_i^{min} - P_i^t)\}|] \quad (2)$$

As most of the fossil fuel based generating units are the main sources of SO_x and NO_x , they have been firmly instructed by the environmental protection agency (EPA) to decrease their production emission levels. This study considered NO_x to be optimally regulated for the environmental aspects. The emission objective function with the inclusion of the valve-point effect can be represented as [26]:

$$f_{emc}(P_i^t) = \sum_{i=1}^{N_G} [(\alpha_i + \beta_i P_i^t + \gamma_i (P_i^t)^2) + \eta_i \exp(\delta_i P_i^t)] \quad (3)$$

In order to evaluate the total cost of generation for the CEED problem the two independent cost functions can be combined by means of a price penalty factor which converts the multi-objective function into a single-objective term as follows [44]:

$$F_{ct}(P_i^t) = f_{gc}(P_i^t) + h_i^{max-max} \times f_{emc}(P_i^t) \quad (4)$$

$$F_{ct}(P_i^t) = \sum_{i=1}^{N_G} (a_i + b_i P_i^t + c_i (P_i^t)^2) + |d_i \times \sin\{e_i \times (P_i^{min} - P_i^t)\}| + h_i^{max-max} \times \sum_{i=1}^{N_G} (\alpha_i + \beta_i P_i^t + \gamma_i (P_i^t)^2) + \eta_i \exp(\delta_i P_i^t) \quad (5)$$

where $h_i^{max-max}$ denotes the price penalty factor (PPF) in dollar per hour. The PPF is the ratio between the maximum generation cost function and the maximum emission objective function, where it can be written as [45]:

$$h_i^{max-max} = \frac{(a_i + b_i P_i^{max} + c_i (P_i^{max})^2) + |d_i \times \sin\{e_i \times (P_i^{min} - P_i^{max})\}|}{(\alpha_i + \beta_i P_i^{max} + \gamma_i (P_i^{max})^2) + \eta_i \exp(\delta_i P_i^{max})} \quad (6)$$

In a general form the proposed CEED objective function can be rewritten as follows:

$$F_{ct}(P_i^t) = \omega_1 \times f_{gc}(P_i^t) + \omega_2 \times h_i^{max-max} \times f_{emc}(P_i^t) \quad (7)$$

where the ω_1 and ω_2 are the weighting factors of the proposed formulation, in such a way that:

- (1) $\omega_2 = 0$ for the pure economic dispatch without the consideration of emission cost.
- (2) $\omega_1 = 0$ for the pure emission dispatch without the consideration of generation cost.
- (3) ω_1 and $\omega_2 = 1$ for the combined environmental economic dispatch (we have considered this combination).

Subject to the following constraints:

The first set of constraints is related to the systematic constraints which are required to be maintained.

Power balance equality constraint:

$$\sum_{i=1}^{N_G} P_i^t = P_D^t \quad (8)$$

The total generation should be able to satisfy the given load demand at any interval, where P_D^t represents the total system load demand at interval t .

Inequality constraints of the generators: For the safety purposes of the generating units as well as the stable operation of the system, all the generating units are firmly limited to operate within their minimum and maximum generation capacity; accordingly, the inequality constraint can be stated as follows:

$$P_i^{min} \leq P_i^t \leq P_i^{max} \quad \text{for } i = 1, 2, 3 \dots N_G \quad (9)$$

The second set of constraints is associated with the physical constraints of the generating units which are required to be strictly upheld.

Ramp rate limits: In CEED formulation, the power output is commonly presumed to be regulated efficiently and instantly. In the real practices, ramp rate limit confines the operating range of all the generating units within two independent intervals [46]; (1) as generation increases and (2) as generation decreases.

$$\max(P_i^{min}, P_i^0 - DR_i) \leq P_i^t \leq \min(P_i^{max}, P_i^0 + UR_i) \quad (10)$$

subject to

$$(1) \quad P_i^t - P_i^0 \leq UR_i \quad (11)$$

$$(2) \quad P_i^0 - P_i^t \leq DR_i \quad (12)$$

Prohibited operating zone (POZ): Modern generating units with the inclusion of the valve-point effect have several prohibited operating zones (POZs) which impose a number of discontinuities in their power generation output [46]. Consequently, in practical operation, POZs splits the operating range among minimum and maximum generation limits into fragmented convex subsections. The practical operating zones can be expressed as:

$$\begin{cases} P_i^{min} \leq P_i^t \leq P_{i,1}^L \\ P_{i,m-1}^U \leq P_i^t \leq P_{i,m}^L \quad m = 2, \dots, N_i^{PZ}; \forall i \in \psi \\ P_{i,N_i^{PZ}}^U \leq P_i^t \leq P_i^{max} \end{cases} \quad (13)$$

Spinning reserve: A minimum system spinning reserve is required to be considered to satisfy the system load demand and be responsible for any frequency changes due to load fluctuations in real-time systems [47].

$$\sum_{i \in \Psi} S_i^t \geq S_R \quad (14)$$

where

$$S_i^t = \min\{P_i^{max} - P_i^t, S_i^{max}\} \quad \forall i \in (\Psi - \psi) \quad (15)$$

$$S_i^t = 0 \quad \forall i \in \psi \quad (16)$$

The spinning reserve requirement should be carried out by the units without POZs, where they have no restriction to regulate their power generation smoothly within the boundaries.

Power balance handling

In order to guarantee that the power balance generation and equality constraint are continuously sustained, the study considered a power balance violation (PBV) method. The PBV can be described as [38]:

$$\sum_{i=1}^{N_G} P_i^t \geq P_D^t \quad (17)$$

subject to

$$PBV = \max\left(1 - \frac{\sum_{i=1}^{N_G} P_i^t}{P_D}, 0\right) \quad (18)$$

As long as PBV is set to zero, the equality constraint has been maintained where the algorithm should only accept the solutions which are capable of holding the following relationship:

$$P_D^t - \sum_{i=1}^{N_G} P_i^t = 0 \quad (19)$$

The study has utilized an evaluation function to speed up the convergence process and obtain the optimum solutions. This approach uses a penalization factor (PF) method to push the answers towards the best possible solution. The proposed method can be expressed as follows:

$$F_{eval} = F_{ct}(P_i^t) \times (1 + PF \times PBV) \quad (20)$$

In this study, the initial value of PF has been considered equal to 1000. Nevertheless, this value could vary up to 1,000,000 based on many factors such as the topology and nature of the problem.

2.3. The third version of cultural algorithm (CA3)

Many decades ago, a number of scientists who were working on the social behavior of people suggested an idea that culture has the ability to be transferred to a population through an inheritance mechanism. In 1994 Reynolds proposed an algorithm based on the cultural model [48]. The cultural algorithm (CA) was established according to the behavior of elite individuals in a certain population, where their behavior is transmitted inherently from generation to generation through motivated operators. The elite group of the population characterizes and regulates the norms [49]. The selection basis of this elite group is based on many factors such as physical appearance, wealth, and knowledge. The knowledge and ideas of those individuals become the most effective

leading factor of the society. Culture or tradition improves from a generation to the next generation in order to make them more conscious and capable of survival. The evolution of a population is a process where the knowledge that has been obtained by elite individuals through generations in the search space (belief space) would be kept to direct the behavior of the other individuals. CA has been implemented based on the two basic components namely the population space and the belief space. The population space is responsible for the storage of an individual's information, and the responsibility of the belief space is to shape and maintain the cultural knowledge during the evolution process. The general framework of CA is depicted in Fig. 2.

CA can be categorized into different versions based on their influence functions. The responsibility of the influence function is to affect the population according to the regulation of beliefs to determine the mutational step size and the direction of changes. Goudarzi et al. [38] proposed four versions for CA, where the third version (CA3) was found as the most efficient version for the CEED optimization. CA3 is based on two knowledge components; the situational knowledge component and the normative knowledge component. The situational knowledge component is in charge of finding the best possible solution in a generation, and is formulated as [38]:

$$S(t + 1) = \{\hat{y}(t + 1)\} \quad (21)$$

where

$$\hat{y}(t + 1) = \begin{cases} \min_{l=1, \dots, n_B(t)} \{X_l(t)\} & \text{if } f(\min_{l=1, \dots, n_B(t)} \{X_l(t)\}) < f(\hat{y}(t)) \\ \hat{y}(t) & \text{otherwise} \end{cases} \quad (22)$$

subject to

$$X_l(t), \quad l = 1, 2, 3, \dots, n_B(t) \quad (23)$$

$$n_B(t) = \left\lceil \frac{n_{pop} \gamma}{t} \right\rceil, \quad \gamma \in [0, 1] \quad (24)$$

where

- $n_B(t)$ is the number of selected individuals for forming the beliefs in a population
- t is the number of iterations (generation)
- n_{pop} is the size of population

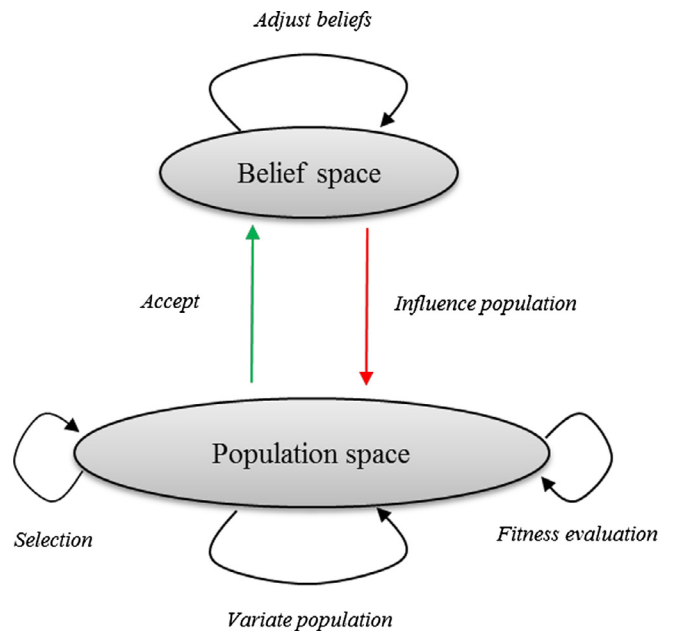


Fig. 2. Conceptual framework of cultural algorithm based on the two spaces.

The normative knowledge is the component which prepares different scales for each individual behavior in order to direct them towards their mutational adjustments. The normative knowledge can be mathematically expressed as:

$$x_j^{min}(t+1) = \begin{cases} x_{ij}(t) & \text{if } x_{ij}(t) \leq x_j^{min}(t) \text{ or } f(X_i(t)) < L_j(t) \\ x_j^{min}(t) & \text{otherwise} \end{cases} \quad (25)$$

For updating the $L_j(t)$

$$L_j(t+1) = \begin{cases} f(X_i(t)) & \text{if } x_{ij}(t) \leq x_j^{min}(t) \text{ or } f(X_i(t)) < L_j(t) \\ L_j(t) & \text{otherwise} \end{cases} \quad (26)$$

$$x_j^{max}(t+1) = \begin{cases} x_{ij}(t) & \text{if } x_{ij}(t) \geq x_j^{max}(t) \text{ or } f(X_i(t)) < U_j(t) \\ x_j^{max}(t) & \text{otherwise} \end{cases} \quad (27)$$

For updating the $U_j(t)$

$$U_j(t+1) = \begin{cases} f(X_i(t)) & \text{if } x_{ij}(t) \geq x_j^{max}(t) \text{ or } f(X_i(t)) < U_j(t) \\ U_j(t) & \text{otherwise} \end{cases} \quad (28)$$

As proposed in this version, the step size would be defined by means of situational knowledge where the changes in direction would be carried out by normative knowledge. CA3 can be described as:

$$\dot{x}_{ij}(t) = \begin{cases} x_{ij}(t) + |\sigma_{ij}(t)N_{ij}(0,1)| & \text{if } x_{ij}(t) < \hat{y}_j(t) \\ x_{ij}(t) - |\sigma_{ij}(t)N_{ij}(0,1)| & \text{if } x_{ij}(t) > \hat{y}_j(t) \\ x_{ij}(t) + \sigma_{ij}(t)N_{ij}(0,1) & \text{otherwise} \end{cases} \quad (29)$$

subject to

$$x_{ij}(t) \sim N_{ij}(x_{ij}(t), \delta_j^2(t)) \quad (30)$$

$$\delta_j(t) = [x_j^{max}(t) - x_j^{min}(t)] \quad (31)$$

$$\sigma_{ij}(t) = \alpha \times \delta_j(t), \quad 0 < \alpha < 1 \quad (32)$$

It is important to mention that, the CA3 is characteristically so fast because it uses two knowledge components (situational knowledge and normative knowledge) as two powerful search engines in the search space to find the optimal solution and it significantly speeds up the convergence process and reduces the running time. Any further details and illustration of the CA3 method can be found in [38].

2.4. Least square support vector machine (LSSVM)

The least square support vector machine (LSSVM) was introduced by Suykens and colleagues and is based on the principal of support vector machine (SVM) [50]. In LSSVM, equality constraints are used as a replacement for inequality constraints through a least square cost function to tackle the difficulty of calculations towards optimal solutions. The proposed cost function can be solved by means of linear Karush-Kuhn-Tucker (KKT) optimality conditions instead of a quadratic programming problem. Consequently, the classical SVM can be reformulated as the following LSSVM cost function [51]:

$$\text{cost function} = \frac{1}{2} w^T w + \frac{1}{2} \gamma \sum_{k=1}^N e_k^2 \quad (33)$$

subject to

$$y_k = w^T \varphi(x_k) + b + e_k, \quad k = 1, 2, 3, \dots, N \quad (34)$$

where

b is the bias

w^T is transposed vector of the output layer

$\varphi(x)$ is the feature map

γ is the adjustable parameter

e_k is the error variable

x_k kth number of input data

y_k kth number of output data

As the vector w can increase to infinite dimensions, making the optimization process cumbersome as in Eq. (33). To overcome this problem, LSSVM has tried to calculate the model in the dual space instead of in the primal space. The Lagrangian solution can be applied as follows [52]:

$$L(w, b, e, a) = \frac{1}{2} w^T w + \frac{1}{2} \gamma \sum_{k=1}^N e_k^2 - \sum_{k=1}^N a_k (w^T \varphi(x_k) + b + e_k - y_k) \quad (35)$$

where a_k denotes the Lagrangian multiplier. The KKT optimality conditions can be expressed by [53]:

$$\begin{cases} \frac{\partial L}{\partial w} = 0 \rightarrow w = \sum_{k=1}^N a_k \varphi(x_k) \\ \frac{\partial L}{\partial b} = 0 \rightarrow \sum_{k=1}^N a_k = 0 \\ \frac{\partial L}{\partial e_k} = 0 \rightarrow a_k = \gamma e_k, \quad k = 1, 2, 3, \dots, N \\ \frac{\partial L}{\partial a_k} = 0 \rightarrow w^T \varphi(x_k) + b + e_k - y_k = 0, \quad k = 1, 2, 3, \dots, N \end{cases} \quad (36)$$

N is the number of data points in the training set $\{x_k, y_k\}_{k=1}^N$, where $x_k \in \mathbb{R}^n$ and $y_k \in \mathbb{R}$. Based on the KKT optimality condition the parameters a_k, e_k, w and b can be computed. These conditions are almost identical to the standard form of SVM as a classifier, apart from the condition $a_k = \gamma e_k$ [52].

To come up with the sparseness property of LSSVM, it is possible to go through the elimination process of w and e where the resultant solution can be expressed as follows:

$$\begin{bmatrix} 0 & 1_v^T \\ 1_v & \Omega + \frac{1}{\gamma} I \end{bmatrix} \begin{bmatrix} b \\ \alpha \end{bmatrix} = \begin{bmatrix} 0 \\ y \end{bmatrix} \quad (37)$$

where

$$y = [y_1; \dots; y_N]$$

$$1_v = [1; \dots; 1_N]$$

$$\alpha = [\alpha_1; \dots; \alpha_N]$$

$$\Omega_{kl} = \varphi(x_k)^T \varphi(x_l) \text{ for } k, l = 1, 2, 3, \dots, N$$

By means of Mercer's condition and the mapping feature the Kernel function can be written as follows [52]:

$$K(x, y) = \sum_{i=1}^N \varphi_i(x) \varphi_i(y), \quad x, y \in \mathbb{R}^n \quad (38)$$

The aforementioned condition is held if and only if, for any function $g(x)$ that $\int g(x)^2 dx$ is finite, there would be one solution.

$$\int K(x, y) g(x) g(y) dx dy \geq 0 \quad (39)$$

As consequence of the above condition the solution of the kernel can be represented as a bullet operator ($K(\cdot, \cdot)$) such that:

$$K(x_k, x_l) = \varphi(x_k)^T \varphi(x_l), \quad k \text{ and } l = 1, 2, 3, \dots, N \quad (40)$$

The LSSVM for the function estimation can be simplified as:

$$y(x) = \sum_{k=1}^N \alpha_k K(x, x_k) + b \quad (41)$$

where α and b are the key parameters to determine. γ is the first adjustable parameter of the LSSVM and as it is a Kernel-based technique, it is required to consider the parameters of kernel functions as another (or second) adjustable parameter of the algorithm. Accordingly, the RBF Kernel function that has been used in this study can be given by [52,53]:

$$K(x, x_k) = \exp\left(-\frac{x_k - x^2}{\sigma^2}\right) \quad (42)$$

The developed LSSVM model has two adjustable parameters (γ and σ^2). The accuracy of the algorithm is highly dependent on its own adjustable parameters. The study utilized CA3 to tune and find the most optimum values of the adjustable parameters to minimize the deviation of the predicted data points. Figs. 3 and 4 represent the network structure and flow chart process of the LSSVM-CA3, respectively.

2.5. Evaluation of prediction performance

The precision of the proposed method (LSSVM-CA3) was examined by means of mean squared error (MSE), root mean squared error (RMSE), normalized root mean squared error (NRMSE) and mean absolute error (MAE). These four performance measurement techniques are extensively used to examine how well a method performs in prediction or fitting of the actual values.

MSE is extensively used to measure the difference between predicted values by a method and actual values. This method compares the mean of squared residuals against the predicted values. RMSE can be assessed by taking a root of the calculated MSE. The evaluated RMSE has a wide range of units with respect to the different test cases. In order to have a uniform comparison capability of RMSE for different methods with diverse units, the non-dimensional form of RMSE known as NRMSE is used. NRMSE is achieved by normalizing the RMSE value to the range of the observed data [54]. Thus the NRMSE values that are closer zero are more desirable, and they represent the better performance of the applied method. The respective formulation for MSE, RMSE and NRMSE can be described as:

$$MSE = \frac{1}{N_G} \sum_{i=1}^{N_G} (P_i^{\text{Actual}} - P_i^{\text{Predict}})^2 \quad (43)$$

$$RMSE = \sqrt{\frac{1}{N_G} \sum_{i=1}^{N_G} (P_i^{\text{Actual}} - P_i^{\text{Predict}})^2} \quad (44)$$

$$NRMSE = \frac{RMSE}{P_i^{\text{max}} - P_i^{\text{min}}} \quad (45)$$

P_i^{Actual} is the actual generation schedule of the units
 P_i^{Predict} is the predicted generation schedule of the units

MAE has also been used to assess the performance of LSSVM-CA3. The evaluation range of MAE is the same as RMSE, however in MAE the values in this study are not expressed in percentage. The mathematical formulation of MAE is as follows [55]:

$$MAE = \frac{1}{N_G} \sum_{i=1}^{N_G} |P_i^{\text{Actual}} - P_i^{\text{Predict}}| \quad (46)$$

3. Results and discussion

In this study, the proposed LSSVM-CA3 method was used to predict and determine the most optimum scheduling of generating units in the real-time system for solving the CEED problem and has been tested on different scenarios. To examine the effectiveness of the proposed method for practical purposes, it has been tested on three different test systems through several considerations test system characteristics. All comparison cases were performed to demonstrate the applicability of the methodology of the study. All the algorithms have been implemented on MATLAB 2015a. They have been executed on a personal computer with the following specifications, Intel® Core™ i5-3210M (3.1 GHz), 6.00 GB RAM (DDR3) and win 8.1 operating system (OS). All the intelligent methods are very sensitive to their adjusting parameters; therefore the study has considered the following values for the compared methods:

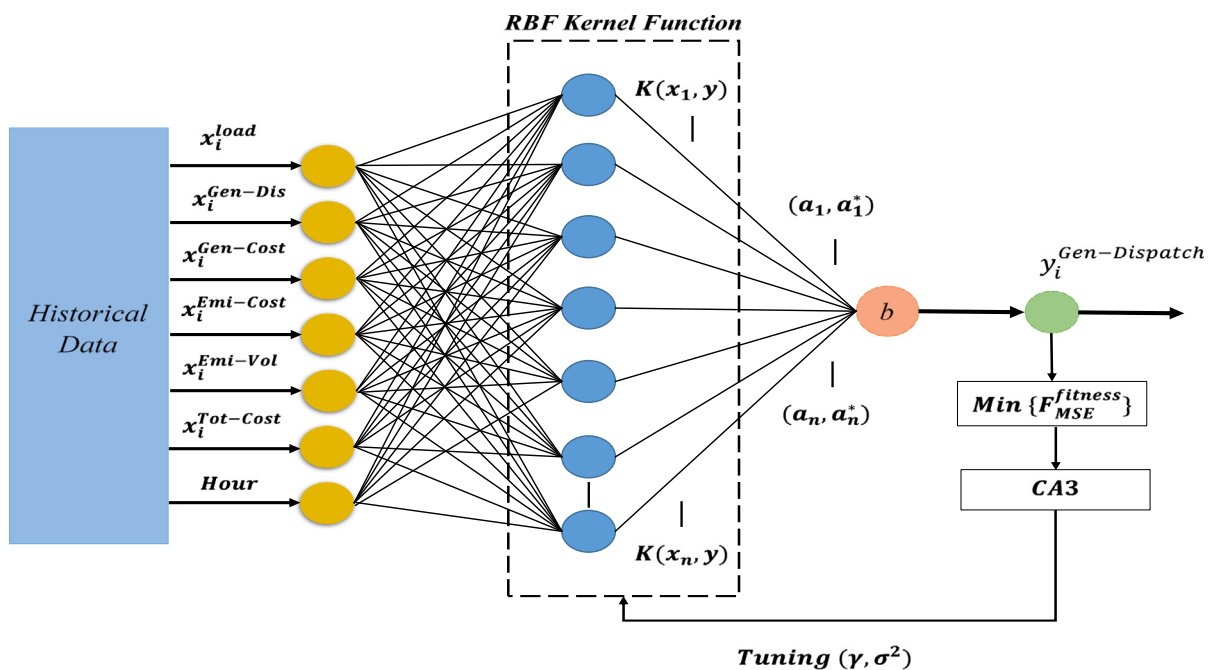


Fig. 3. General network structure of LSSVM-CA3.

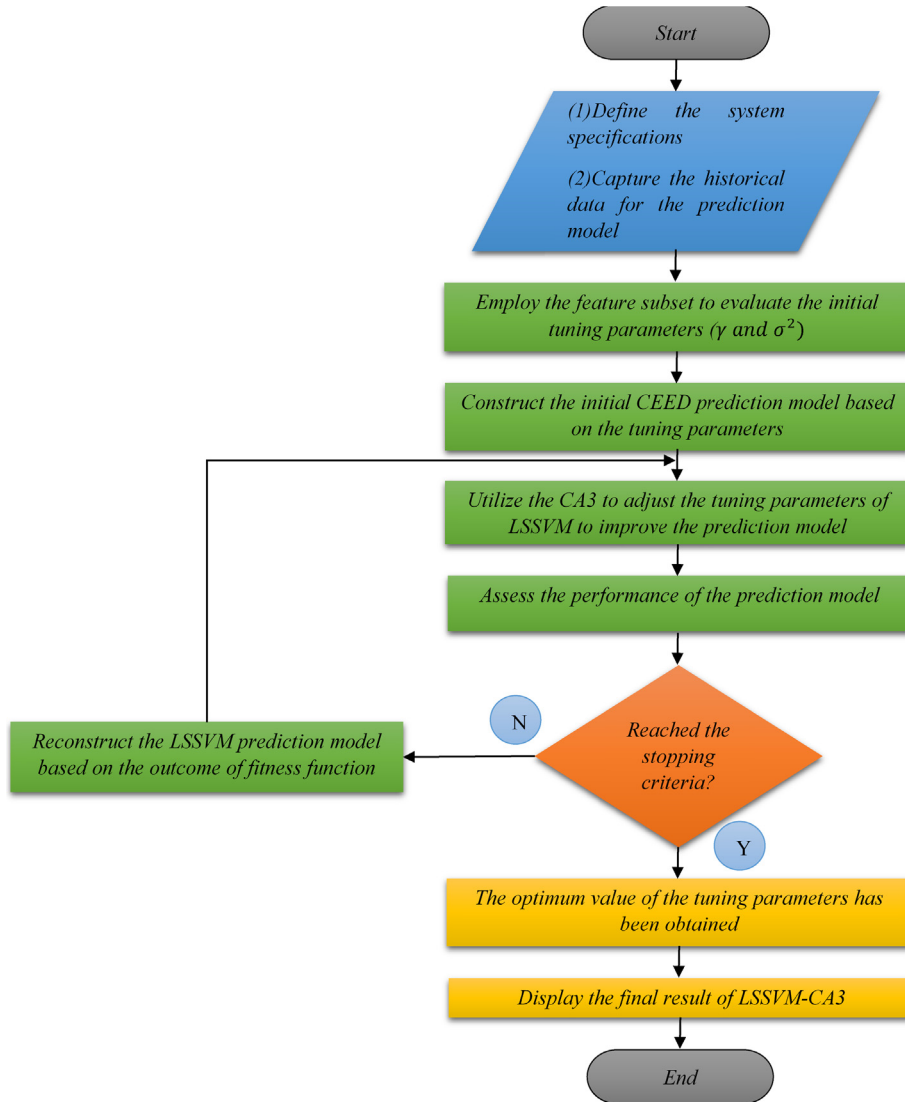


Fig. 4. Flow chart process of LSSVM-CA3.

GA:

- Population size: 50
- Maximum number of iterations: 50
- Crossover probability: 0.8
- Mutation probability: 0.1

PSO:

- Population size: 50
- Maximum number of iterations: 50
- C1 and C2: 2
- Inertia weight: Min = 0.4 and Max = 0.9

ICA:

- Population size: 50
- Maximum number of iterations: 50
- Number of empires: 10
- Selection pressure: 1
- Assimilation coefficient: 1.5
- Revolution probability: 0.05

- Revolution rate: 0.1
- Colonies mean cost coefficient: 0.2

CA3:

- Population size: 50
- Maximum number of iterations: 50
- Acceptance ratio: 0.15
- Strategy parameter: 0.25
- Scaling coefficient: 0.5

The study has considered a daily load curve (24 h load points) according to the capability of each test system for handling of the load demand, while the daily load curves have been specified in each studied case. Daily load curves have been used for training purposes of all predictors. In real practice, by having the historical data of any system over a sufficient period of time and using the maximum likelihood method (MLE) the most probable load points of the system during a day can be determined. Due to the unavailability of data for the loss coefficients in different hours of the day in each test system, the calculation of power loss has not been taken into account. All the required data regarding the test system

specifications are given in the appendix section. As the renewable energy resources (RESs) like wind and solar have an uncertain and intermittent behavior, therefore, they require another mathematical approach to model and forecast their generation behavior before any prediction process regarding the optimal scheduling of the available units, where in this study we assumed all the generating units are running and they are available to be scheduled at any time. Therefore, in the current study, we have not considered any RESs in the studied test cases.

The main focus of the study is to find a fast, intelligent and practical solution for the real-time scheduling of generating units through to CEED problem, not the unit commitment (UC) problem. Therefore, the proposed solution for the real-time CEED problem only deals with the optimal allocation of the load demand among the running units while satisfying the power balance equations and considering the physical operating limits and environmental constraints of generating units.

Almost all of the deterministic mathematical methods are incapable of solving the non-convex problem with discontinuous domains. This study used one of the most recent methods which is widely used in industries and wholesale electricity spot markets to solve the CEED problem with discontinuous operating zones. This method is based on mixed integer quadratic programming (MIQP) while the Branch-and-Bound method through a binary tree with the interior-point algorithm is coupled with MIQP to deal with discontinuous zones [56]. To simulate the same approach of solving the CEED as it is practiced in real-time electricity markets, the study applied MIQP to compute the optimal scheduling of generating units for each hour of the day which was used for a realistic comparison between the proposed method and the current industrial approach in solving CEED as well as the preparation of a database for training purposes.

The calculated database has been divided into two subsets namely, training and testing. To enhance the applicability of the

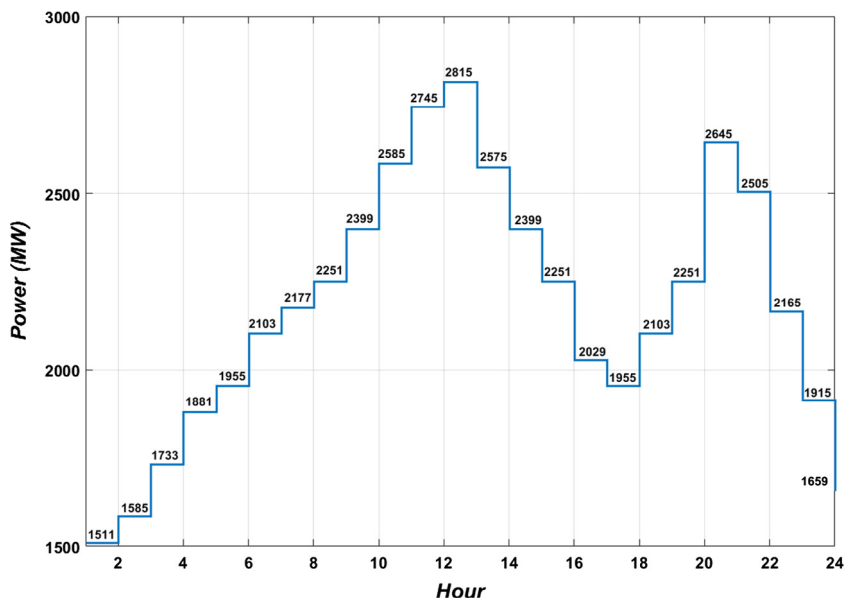


Fig. 5. Daily load curve for 15 units system.

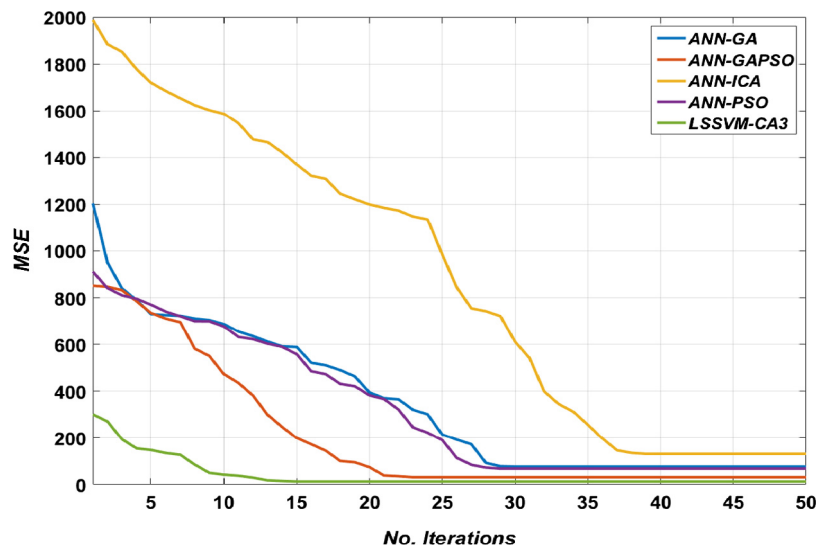


Fig. 6a. Convergence process of LSSVM-CA3 adjusting parameters (first predicted load point, 1600 MW).

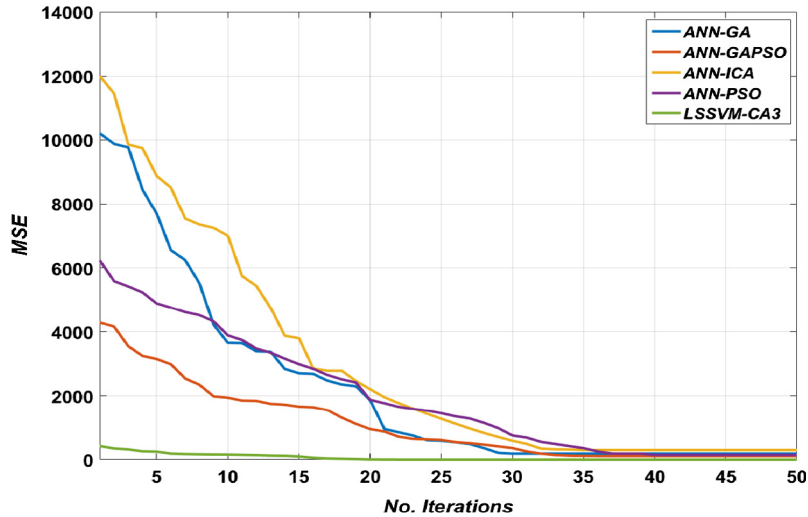


Fig. 6b. Convergence process of LSSVM-CA3 adjusting parameters (second predicted load point, 2475 MW).

model, the entire database has been randomly divided into the following percentages; 80% used for the training set and 20% used for the testing set. The training set was applied to generate the model structure and the testing set was employed to examine the final performance and validity of the proposed model. AS all the compared predictors were coupled with an optimization algorithm for tuning their adjusting parameters, therefore the validation set was not considered. The adjusting parameters of LSSVM (γ and σ^2) are optimized by CA3, while the adjusting parameters of ANN such as input weight matrix (IW), layer weight matrix (LW) and bias vectors (b) have been optimally tuned by GAPSO, PSO, GA and ICA respectively. To investigate the practicality and the robustness of the proposed method it has been compared to four most prominent prediction methods developed namely; ANN-GAPSO, ANN-PSO, ANN-GA and ANN-ICA. The objective function of all prediction methods is to minimize the errors in prediction according to mean squared error (MSE) technique.

In this study, a specific design has been used for the RBF-kernel function to approximate a very precise initial guess based on the input data. The basic kernels have been used as a predefined set of initial guess of the kernel matrices. The utilized kernel learning algorithm operates by inserting the data into a Euclidean space. Thereafter, it searches for a linear relationship between the inserted data points. The inserting is achieved implicitly, by identifying the internal products between each pair of data points in the embedding space. This information is stored in the kernel matrix, which is a symmetric and positive semidefinite matrix that encodes the relative positions of all data points. The determined Kernel matrix helps the SVM to predict a very accurate initial guess which effectively causes a reduction in the initial MSE in the prediction process.

To demonstrate the practicality of the proposed method in the prediction of the generating unit’s schedules, two unknown load points were selected within the generation capacity range. Both of the load points for each test system were selected in a way that

Table 1 Final optimized values for LSSVM-CA3 adjusting parameters (15 units system).

Load point (MW)	γ	σ^2
1600	114.21	3.24
2475	743710.44	68.84

they can distinctly demonstrate the capability of LSSVM-CA3, where the first load point was located in the lower generation range and the second one was picked from a challenging operating area of the generating units, where they have the highest probability of occurrence during a day. For both load points, a number of the scheduling scenarios could be taken into account with regard to the flexibility of the generating units in the least cost operation.

In order to have a unified comparison for all studied cases, the spinning reserve requirement was set as 5% of total load demand as in [57]. The study executed 20 trials for each scenario to produce fair results and consideration of any associated error in calculations, while the maximum number of iterations for all the trials was fixed at 50. Due to the large dimension of the test systems, it is not feasible to present the generators’ dispatches, however, the final evaluations for each scenario have been tabulated as a means of comparison.

3.1. Test case 1

This case attempted to demonstrate the efficiency of the proposed method of study to find the optimal scheduling of generating units without using the CEED method. For this purpose, the proposed method was applied to find the optimal scheduling of a 15 units test system, where the system specifications are available in Appendix A. The effect on the total generation cost of ramp rate

Table 2 Comparison of the obtained results for MSE (15 units system).

	Min	Avg	Max	Avg elapsed time (s)
1600 MW				
LSSVM-CA3	12.72	49.74	128.38	0.13
ANN-GAPSO	31.38	278.08	737.69	15.24
ANN-PSO	67.97	274.86	803.64	2.46
ANN-GA	76.76	280.31	911.17	2.15
ANN-ICA	131.20	402.16	1554.21	6.22
MIQP	35.36
2475 MW				
LSSVM-CA3	0.78	40.27	102.43	0.14
ANN-GAPSO	109.07	731.67	3338.70	17.57
ANN-PSO	144.07	290.35	774.21	2.85
ANN-GA	186.12	520.05	976.64	3.39
ANN-ICA	299.15	579.99	1255.03	5.86
MIQP	35.75

limits, spinning reserve requirement and prohibited operating zones were considered. Fig. 5 depicts the daily load curve for this test system, while the highest and lowest load of the day were equal to 1511 and 2815 MW, respectively. The hourly load, total

generation cost of each hour and their respective generator schedules have been used as inputs for training and constructing the initial model. MIQP has been used to find the most optimum schedules for every given load point of the day. Two random load

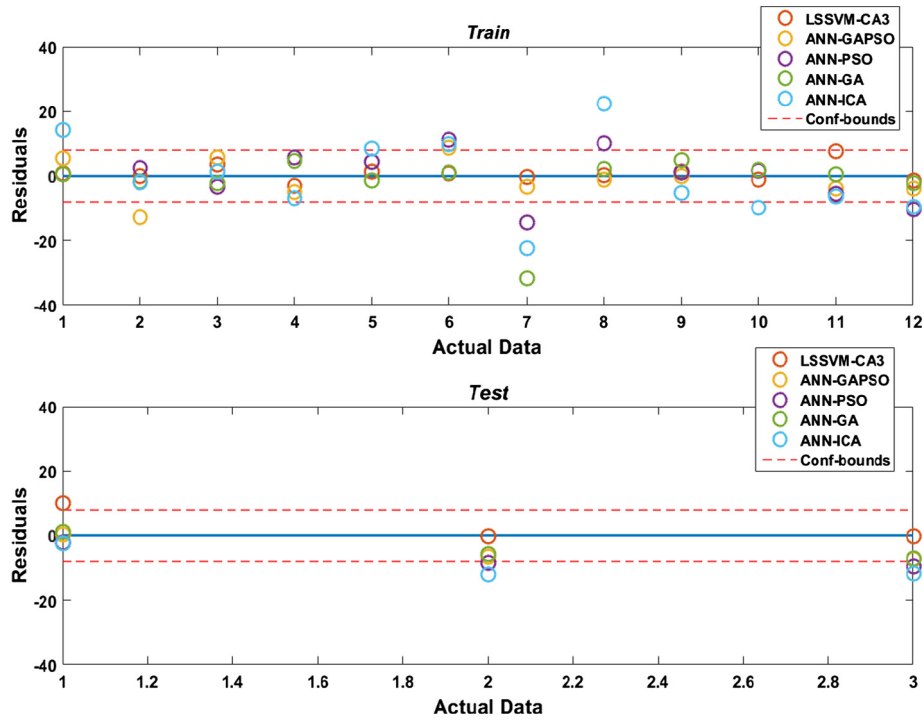


Fig. 7a. Residual representation for the first predicted load point (1600 MW).

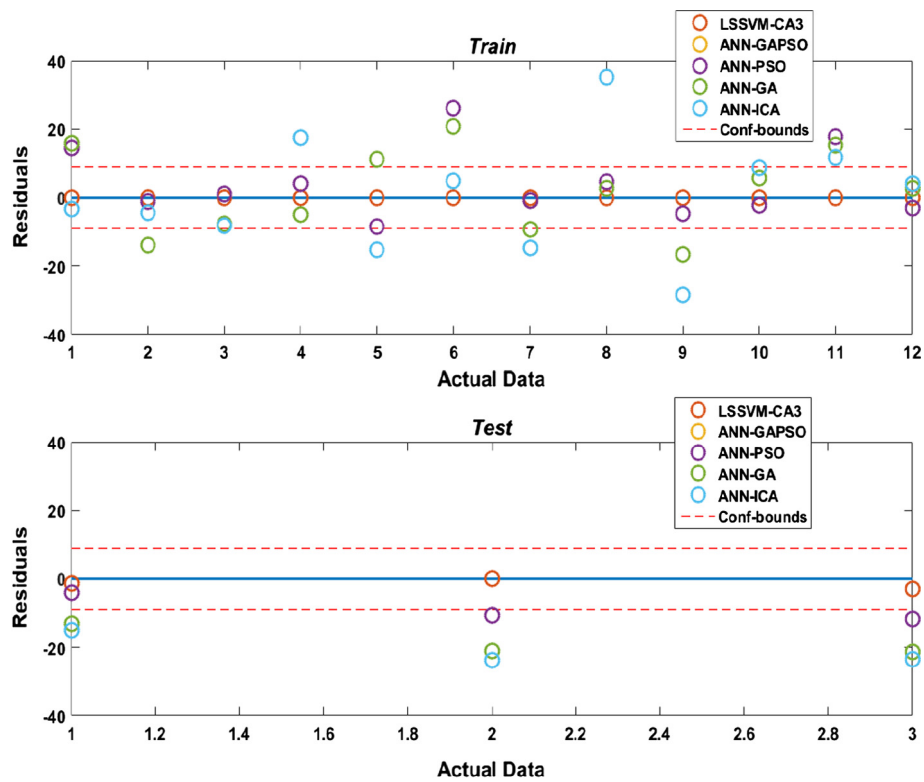


Fig. 7b. Residual representation for the second predicted load point (2475 MW).

points (1600 and 2475 MW) among the given load points have been selected to be found by LSSVM-CA3 and the other methods, where for comparison purposes the schedules of these two load points have been found by MIQP. The process of convergence of the adjusting parameters of all predictor methods in order to minimize the MSE for both the selected load points are shown in Figs. 6a and 6b.

As it can be seen from Figs. 6a and 6b, the proposed algorithm (LSSVM-CA3) has reached to its optimum level in less than 17 iterations for the both load points, whereas the other methods have reached in closer to 30th iterations. Table 1 tabulates the final values of the adjusting parameters for the LSSVM-CA3. Table 2 tabulates the maximum cost, average cost, minimum cost, and average elapsed time for all the compared methods. For simplicity of comparison, the elapsed time of each method was calculated for the average time of all 20 trials. From Table 2, it is clear that the LSSVM-CA3 has obtained the lowest average and minimum total generation cost in comparison to the other methods with the lowest processing time.

Figs. 7a and 7b show the residuals representation of the methods for both the load points compared to the calculated actual values using MIQP. For accurate evaluation of the predictions, the residual set has been divided into two subsets; train and test. In order to have a precise assessment of residual behaviors, the confidence bound has been set as 25% of the highest deviation from the actual generating units' schedules. Placement of more residual values within the confidence bound and closer to the actual data line (actual generator schedules calculated by MIQP) demonstrates the higher accuracy of the method. The LSSVM-CA3 represents the highest accuracy for both load points in comparison to the other methods. For the first load point, the placement of the residuals for the different subsets are 91.67% for the training phase, 66.67% for the testing phase with a total of 86.67%. In the case of the second selected load point, the performance of the proposed method is absolutely outstanding by having 100% accuracy of prediction placement within the confidence bound, where the second best method is ANN-GAPSO by having 66.67% placement inside the confidence bound in total.

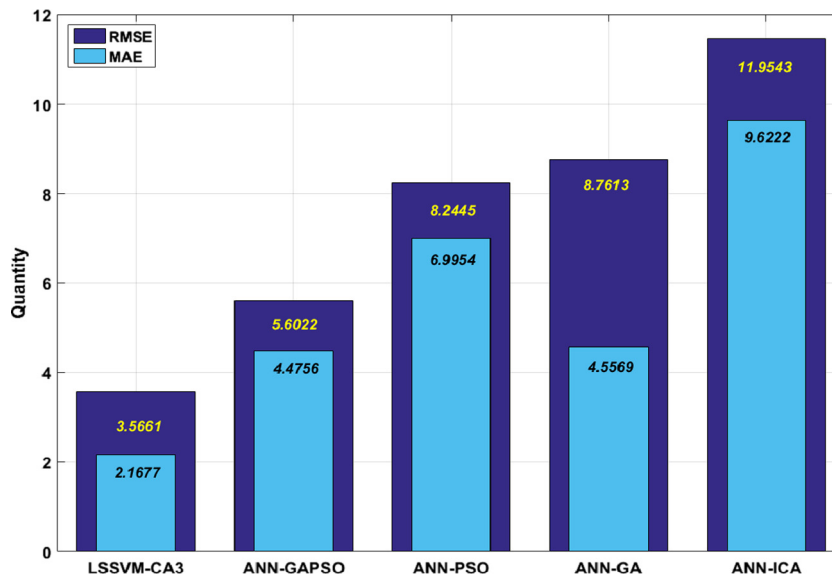


Fig. 8a. Evaluation of RMSE and MAE for the first predicted load point (1600 MW).

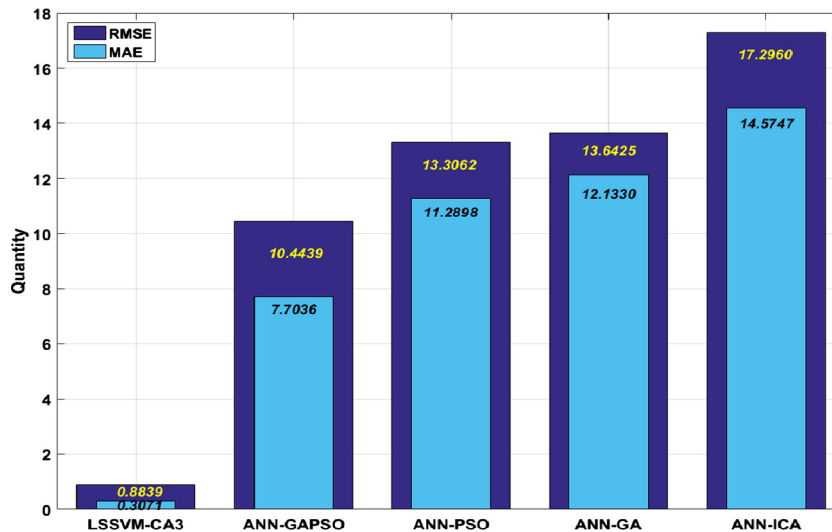


Fig. 8b. Evaluation of RMSE and MAE for the second predicted load point (2475 MW).

The performance of all predictors are examined by two other statistical methods namely; root mean squared error (RMSE) and mean absolute error (MAE). From Figs. 8a and 8b, it is evident that the LSSVM-CA3 has achieved considerably lower values for both predicted load points.

3.2. Test case 2

In order to validate the efficiency of the proposed method of study on a larger test system, LSSVM-CA3 is applied to 40 units system. The system specification is available in Appendix B. In this case, the effect of ramp rate limits, spinning reserve requirement, valve-point loading and emission volume, as well as its associated

costs, were considered. The daily load curve for the 40 units system is shown in Fig. 9. Fig. 10 shows the three-dimensional representation of total generation cost for the entire given load curve. The peak load of the day is equal to 10,500 MW. The hourly load, total generation cost, emission volume, emission cost, generation cost of each unit and generator schedules have been used as the training inputs for the test case. The two random load points for the prediction purposes was 7550 and 8260 MW. The load point 8260 MW, presented a challenging load point due the characteristics of this test system because there are a number of generators which have the same generation capacity to be scheduled while they have a very different behavior from their emission volume production. This situation created a considerable challenge for the convergence

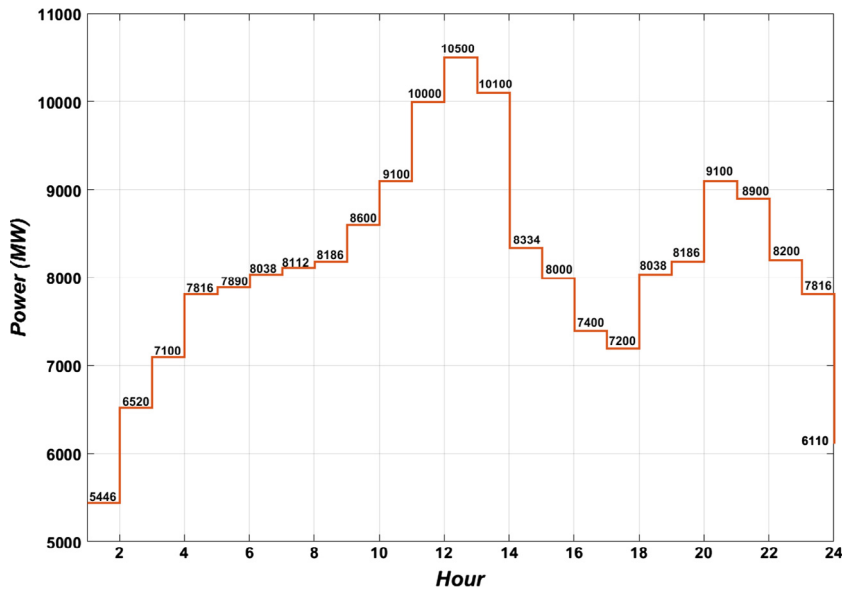


Fig. 9. Daily load curve for 40 units system.

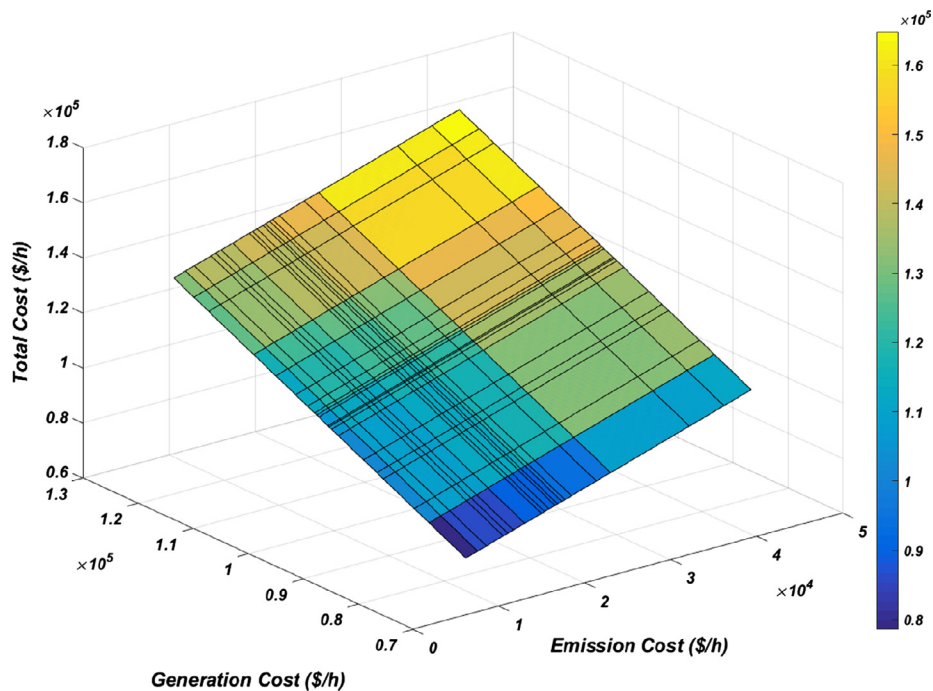


Fig. 10. Total generation cost of the day for the 40 units system.

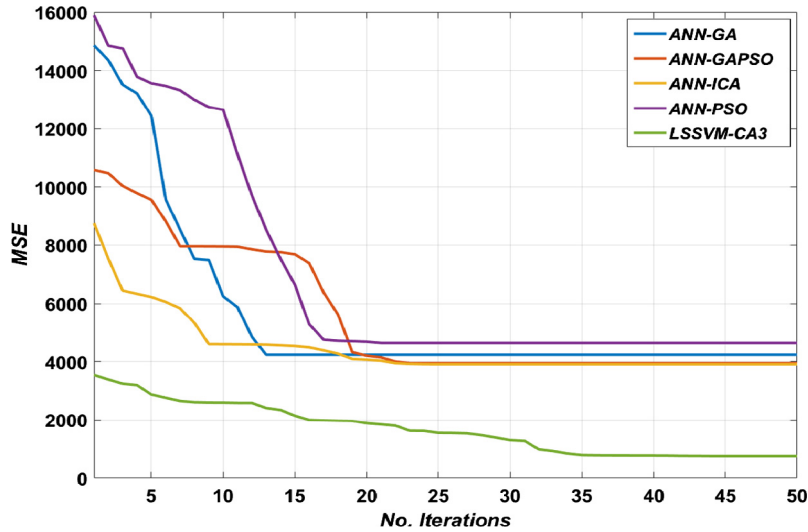


Fig. 11a. Convergence process of LSSVM-CA3 adjusting parameters (first predicted load point, 7550 MW).

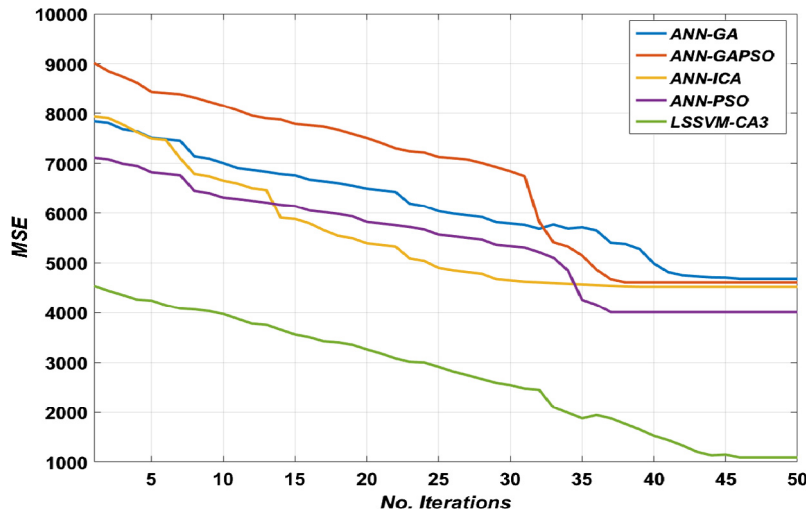


Fig. 11b. Convergence process of LSSVM-CA3 adjusting parameters (second predicted load point, 8260 MW).

Table 3
Comparison of the obtained results for MSE (40 units system).

	Min	Avg	Max	Avg elapsed time (s)
<i>7550 MW</i>				
LSSVM-CA3	753.99	1740.69	2252.17	1.55
ANN-GAPSO	3947.07	5742.35	9243.48	18.46
ANN-PSO	4638.41	5954.64	7907.23	4.66
ANN-GA	4236.25	6578.47	12339.93	4.88
ANN-ICA	3907.89	5244.00	7734.23	12.56
MIQP	3.25
<i>8260 MW</i>				
LSSVM-CA3	1090.65	1951.57	3088.06	1.29
ANN-GAPSO	4612.22	5971.63	8016.21	17.33
ANN-PSO	4009.55	5272.94	6155.87	5.15
ANN-GA	4683.69	5503.89	7366.83	5.23
ANN-ICA	4542.76	5792.29	7766.02	12.86
MIQP	3.83

Table 4
Final optimized values for LSSVM-CA3 adjusting parameters (40 units system).

Load point (MW)	γ	σ^2
7550	26.88	7.40
8260	74390.99	5.99

of the optimization algorithm. The comparison between the proposed method and the other predictors during the convergence process of adjusting parameters is depicted in Figs. 11a and 11b.

It is evident that by the consideration of the effect of valve-point loading on the generation and emission objective function for all the generating units of this test system, all the prediction methods faced a considerable challenge in finding the optimum values of the adjusting parameters. As it can be seen, most of them have reached their final values towards 50 iterations, whereas for the second load point (8260 MW) most of them reached their final point marginally before the 40th iteration. ANN-ICA showed a better performance in comparison with the other methods of ANN, where it achieved the second rank in the first load point after LSSVM-CA3 and third rank after ANN-PSO in the second load point. Nonetheless, the LSSVM-CA3 achieved the lowest values of MSE in comparison to the other methods for both load points. It can be inferred that the performance of all other predictors are highly reliant on the nature of the problem, unlike LSSVM-CA3 which

has shown superior performance in all studied cases. The detailed MSE results of the 40 unit system are shown in Table 3. Table 4 tabulates the final values of the adjusting parameters for the LSSVM-CA3. From Table 3, it is apparent that the proposed method

achieved the lowest MSE in comparison to other techniques, where the minimum MSE for the first and the second load points are 753.9947 and 1090.6507, respectively. However, from the results of Table 3, it can be inferred that, by increasing the level of

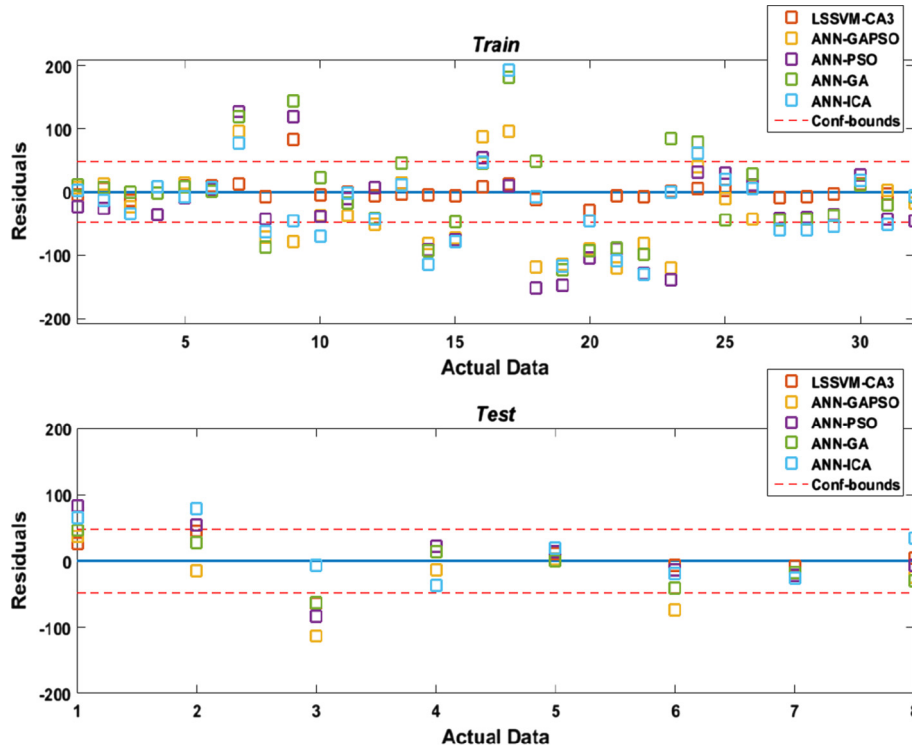


Fig. 12a. Residual representation for the first predicted load point (7500 MW).

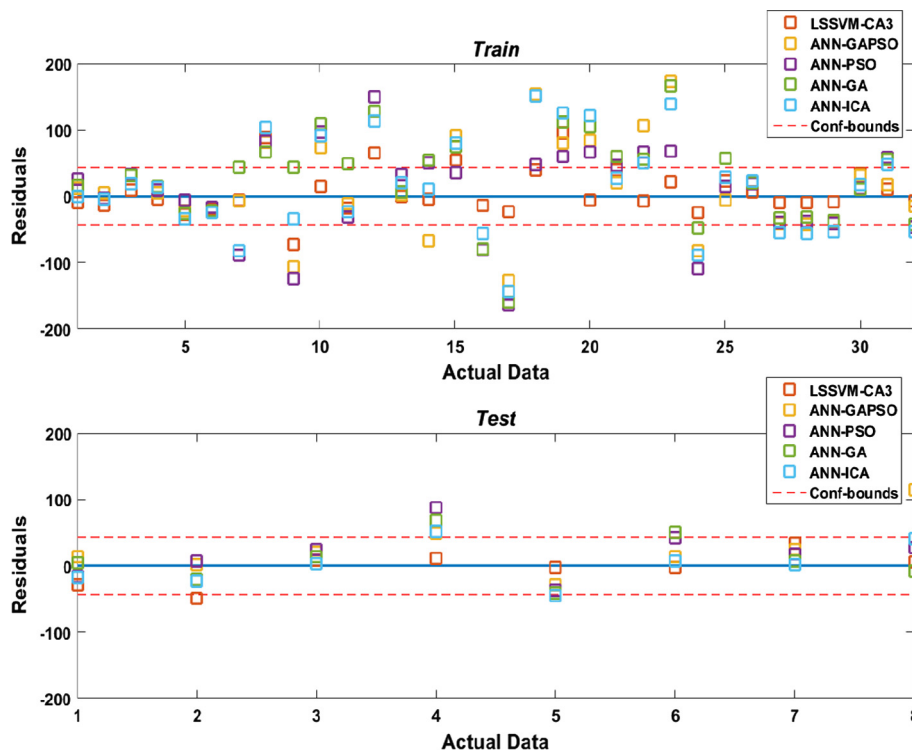


Fig. 12b. Residual representation for the second predicted load point (8260 MW).

nonlinearity which has been imposed by the system because of the valve-point effect the MSE values for all the methods have been considerably increased.

By increasing the dimension of the test system it was expected that there would be a considerable increment in run-time of MIQP, however this was not the case. The reason was that the generating units did not have any POZs, therefore a simple MIQP has been used to find the optimal solutions. That is why, the MIQP run-time has been significantly reduced. The physical considerations for this test system are less realistic in comparison to real world practice due to the absence of the POZs. The main aim of investigating this test system was to analyze the behavior and the processing time of the prediction methods in absence of the POZs. The LSSVM-CA3 method maintained the very quick and efficient run-time when compared to the previous case.

Figs. 12a and 12b exhibit the residuals representation of the methods for both the load points. The LSSVM-CA3 obtained the highest accuracy for both the load points. For the first load point (7550 MW) the placement of the residuals within the confidence bound is illustrated as follows; 93.75% for training phase, 87.5% for the testing phase and with a total of 92.50%. In the case of the second load point, the residual placement results are listed as; 84.38% for training phase, 87.50% for the testing phase and in total 85.00%.

Figs. 13a and 13b compare the performance of all predictors for RMSE and MAE error estimation. After LSSVM-CA3 which obtained the lowest errors for both load points, the ANN-ICA and ANN-PSO reached to the lowest errors in the first and second load points, respectively. This incident confirms that the performance of the methods depends on the topology of the problem; however, again

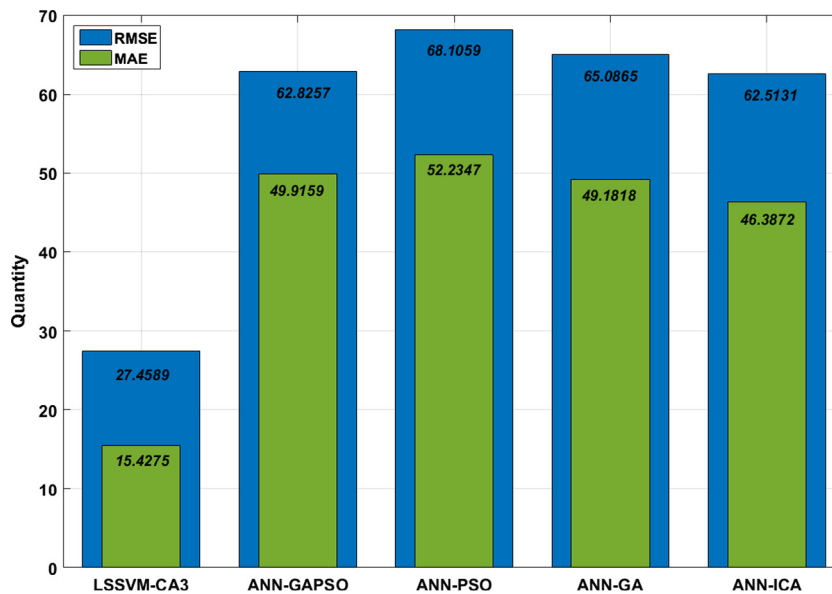


Fig. 13a. Evaluation of RMSE and MAE for the first predicted load point (7500 MW).

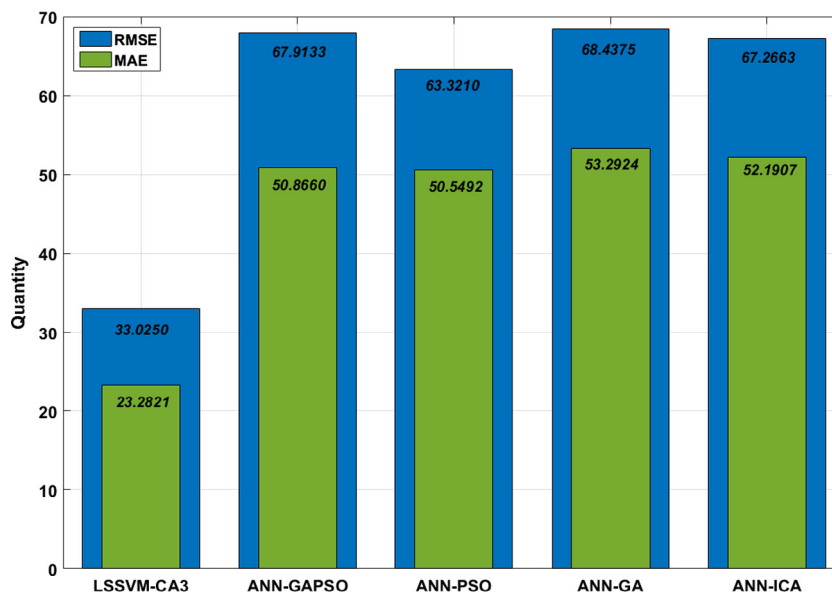


Fig. 13b. Evaluation of RMSE and MAE for the second predicted load point (8260 MW).

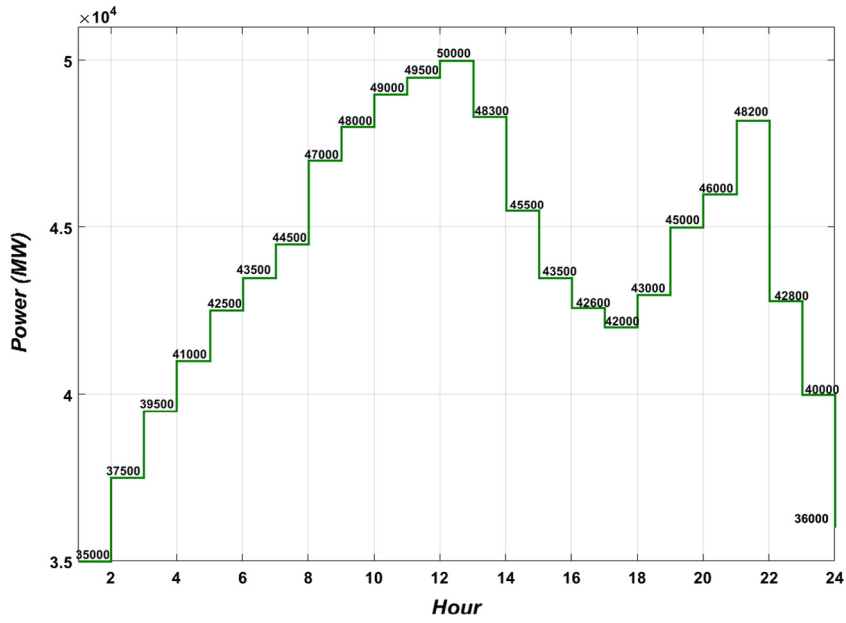


Fig. 14. Daily load curve for 140 units system.

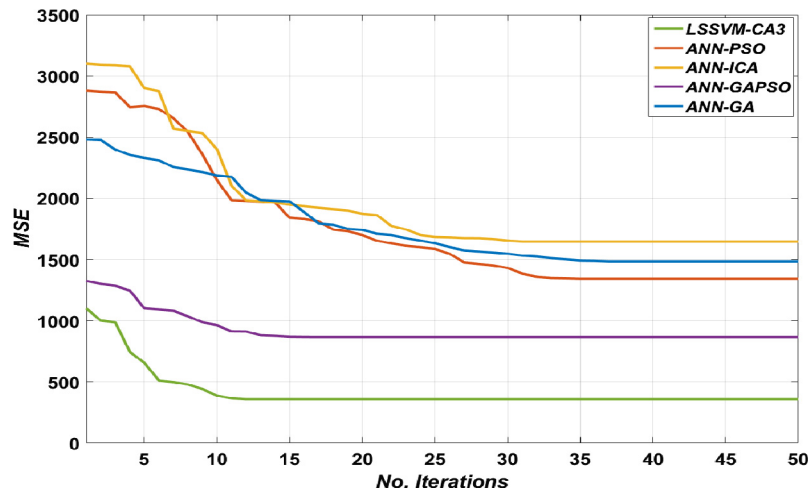


Fig. 15a. Convergence process of LSSVM-CA3 adjusting parameters (first predicted load point, 36,500 MW).

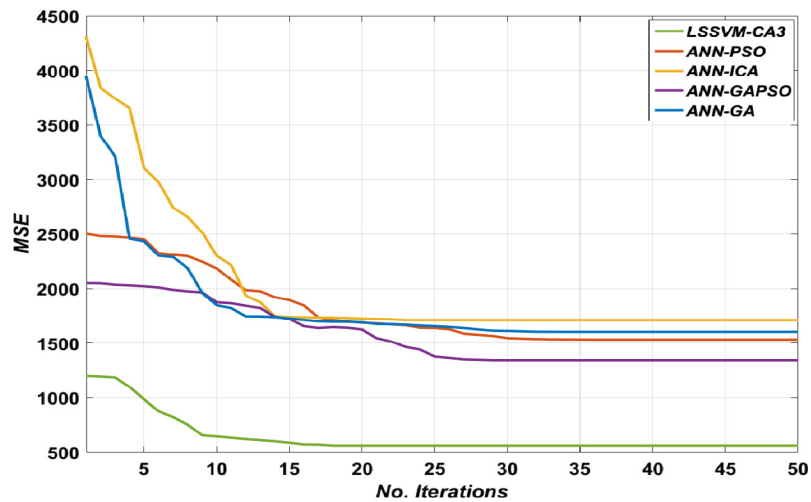


Fig. 15b. Convergence process of LSSVM-CA3 adjusting parameters (second predicted load point, 41,800 MW).

Table 5
Final optimized values for LSSVM-CA3 adjusting parameters (140 units system).

Load point (MW)	γ	σ^2
36,500	63381.17	26822.02
41,800	23.56	4.71

Table 6
Comparison of the obtained results for MSE (140 units system).

	Min	Avg	Max	Avg elapsed time (s)
<i>36,500 MW</i>				
LSSVM-CA3	353.14	370.99	398.54	1.87
ANN-GAPSO	865.48	1384.96	1697.52	46.85
ANN-PSO	1344.16	1604.88	2170.54	7.25
ANN-GA	1483.91	1723.95	1941.63	8.13
ANN-ICA	1646.36	1876.39	2850.12	39.24
MIQP	289.33
<i>41,800 MW</i>				
LSSVM-CA3	512.04	870.79	1191.83	1.95
ANN-GAPSO	1349.40	1644.57	2043.18	47.82
ANN-PSO	1532.17	1866.91	2435.48	7.84
ANN-GA	1603.25	1933.66	3020.83	8.77
ANN-ICA	1711.14	2063.72	2701.94	41.36
MIQP	312.41

the LSSVM-CA3 regardless of the system characteristics exhibited precise prediction of the generator’s schedules.

3.3. Test case 3

This test case was performed to verify the robustness and practicality of the proposed method on a large-scale power system with the higher dimension of complexity. The LSSVM-CA3 was employed on a 140 unit system to predict the optimum scheduling of the generating units, where the system specification is available

in Appendix C. This test system was based on a realistic Korean power system, which consists of 140 thermal units such as coal, LNG, LNG-CC, nuclear and oil. The effect of ramp rate limits, prohibited operating zones, spinning reserve requirement, and valve-point loading were taken into account as the physical constraints of the generating units. Fig. 14 depicts the daily load curve of this test system. For this system, the maximum generation capacity to satisfy the load demand was equal to 50,000 MW and the minimum is set to 35,000 MW. The hourly load, total generation cost, generation cost of each unit with the consideration of the valve-point effect cost and the generator schedules have been utilized as the training inputs. In this case, 36,500 and 41,800 MW are selected as the random load points to be predicted by the methods. This test system had a substantial non-linearity and non-convexity in its operating zones due to its characteristics which made the optimization process cumbersome for any methods to evaluate the most optimum solution for any given load point.

Figs. 15a and 15b illustrate the convergence process of adjusting parameters of the prediction methods to achieve the least possible errors. The methodology of the study successfully acquired the lowest MSE for both load points in comparison to the other methods. For both load points, the LSSVM-CA3 reached its final optimum level in less than 17th iterations while the other methods took approximately 30 iterations to reach their final stage of optimization of their adjusting parameters. Table 5 shows the final values of adjusting parameters for the LSSVM-CA3 for both load points.

The comprehensive investigation of the methods for evaluating MSE are found in Table 6, where LSSVM-CA3 obtained the lowest minimum of MSE in comparison to the other methods with 353.1383 and 512.0360 for the first and second load point, respectively. It can be observed from Table 6, the proposed method has accomplished the prediction in less than 2 s with a noticeable accuracy for both selected load points while the other methods

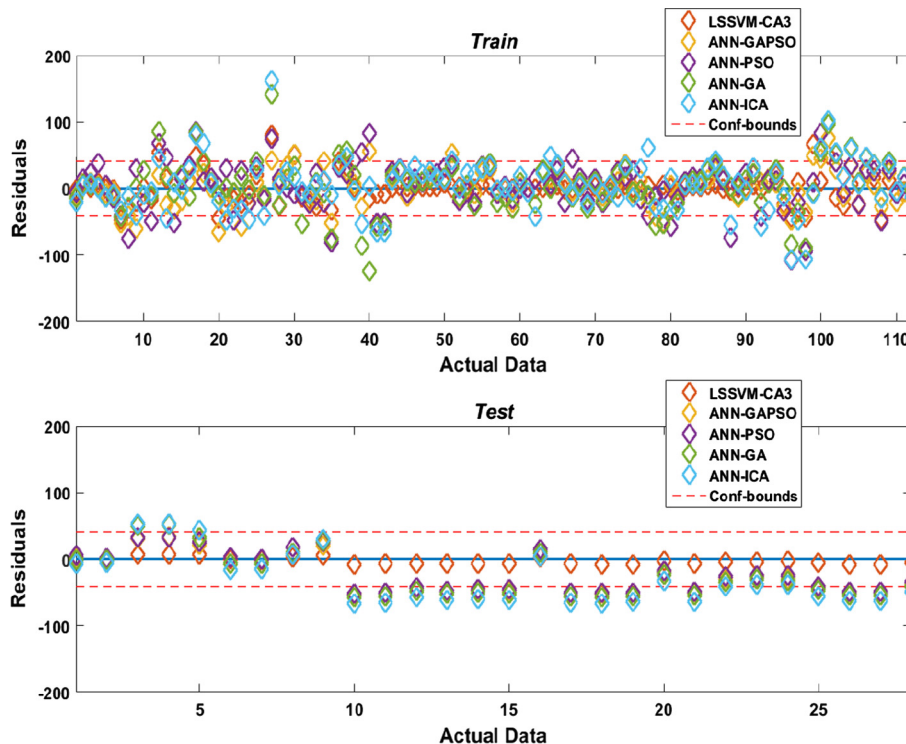


Fig. 16a. Residual representation for the first predicted load point (36,500 MW).

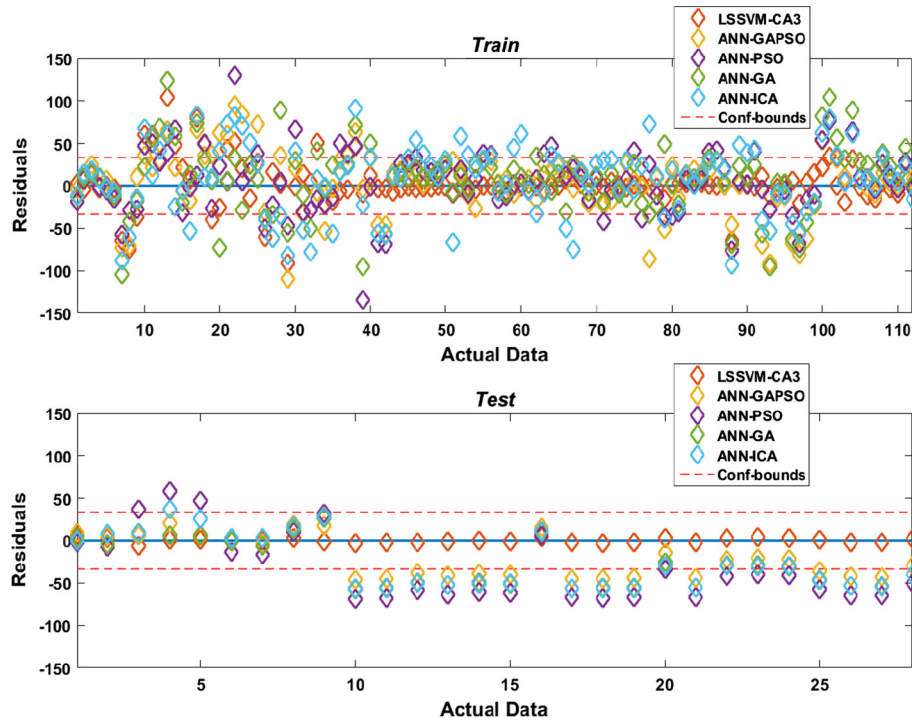


Fig. 16b. Residual representation for the second predicted load point (41,800 MW).

could not achieve even 50% of its precision within approximately 4–23 times higher processing time. Table 6 demonstrates the superior performance of the proposed method through to accurate prediction of generator schedules with a large-scale of complexity. ANN-GPSO, ANN-PSO, ANN-GA and ANN-ICA have a significant poor performance when compared to LSSVM-CA3. It is significant to mention that, even if considering a larger system, the proposed algorithm is able to determine the optimal allocation of power among the generating units in a very fast processing time, which indicates the applicability of the proposed method for real-time management and operation of the power grid where the system

operator needs to run several scenarios with respect to the fluctuations of load demand and demand response programs.

Most of the previous studies in this area discussed the outlier predictions through the leverage method to show the notable performance of their methods. In this study, a strong focus on the placement of the predictions within the confidence bound as well as their concentration around the horizontal actual data line have been considered, as it can indicate a good agreement between the predictions and the actual values. Figs. 16a and 16b describe the residual placement of the predictions. LSSVM-CA3 acquired the best results for both load points, where the placement of the

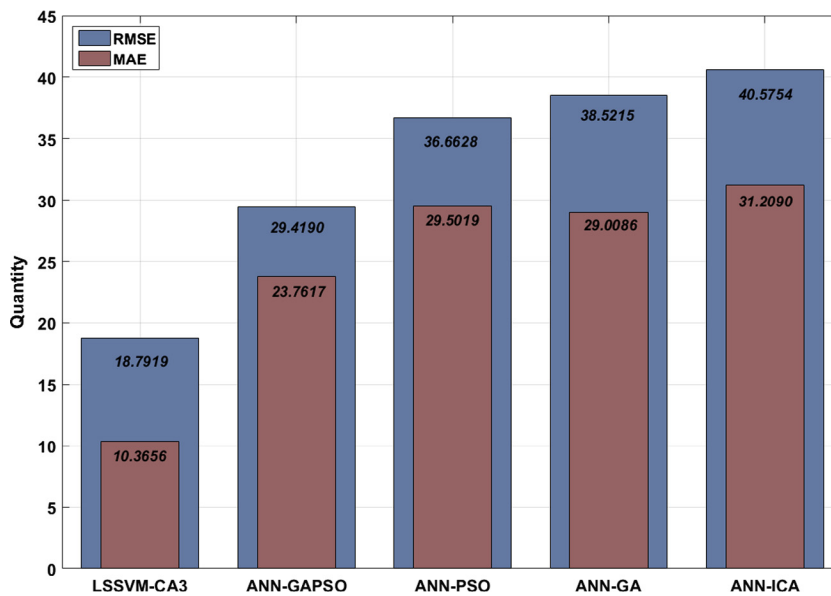


Fig. 17a. Evaluation of RMSE and MAE for the first predicted load point (36,500 MW).

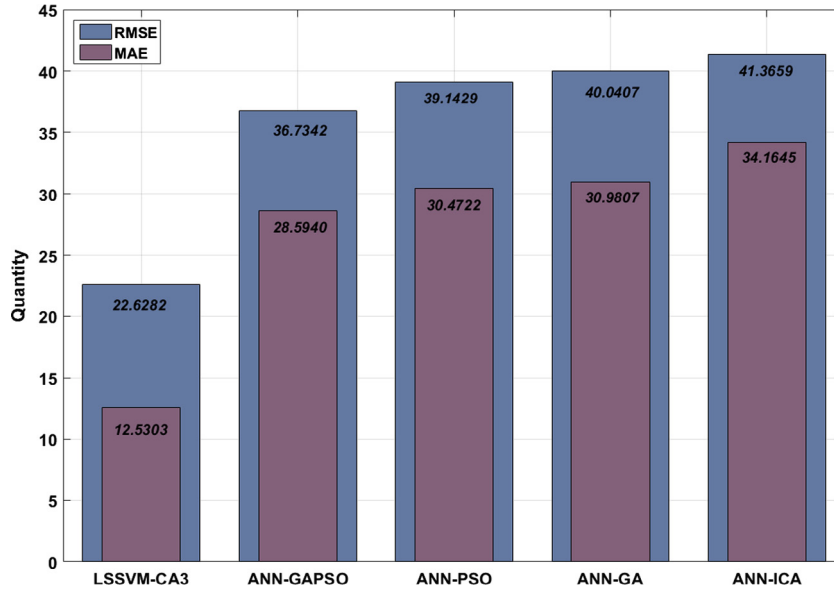


Fig. 17b. Evaluation of RMSE and MAE for the second predicted load point (41,800 MW).

residuals within the confidence bound for the first load point (36,500 MW) is as the following order; 90.18% for the training, 100% for the testing with a total of 92.14%. In the case of the second load point (41,800 MW), the detailed assessment of the residual placement was as follows; 83.93% for the training, 100% for the testing and in total 87.14%. It is evident that even by enlarging

the test system and considering a number of constraints, the residuals have been located considerably close to the actual data line.

The RMSE and MAE comparison for all prediction methods is shown in Figs. 17a and 17b. The LSSVM-CA3 demonstrated excellent performance for load points, where the minimum values of MAE are respectively; 10.37 and 12.53 for the first and second load

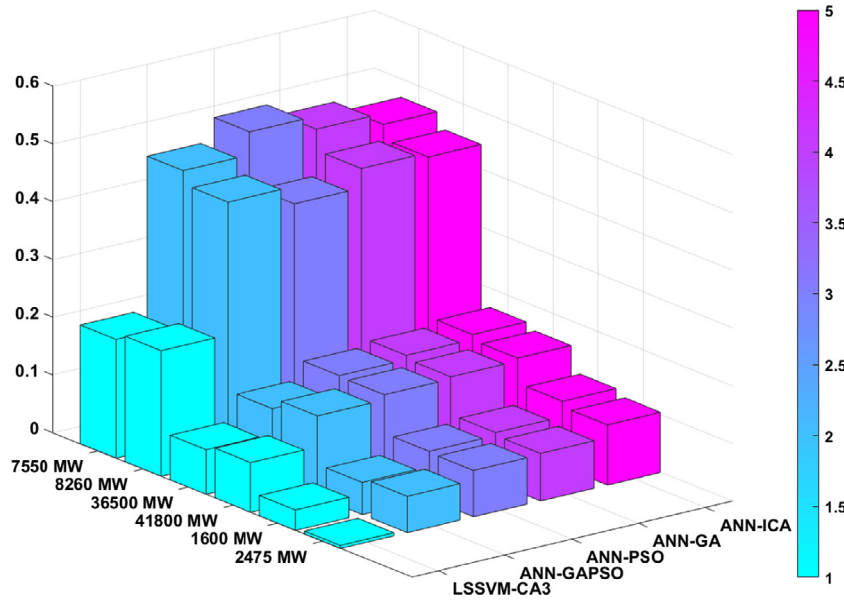


Fig. 18. Evaluation of NRMSE for all the studied cases.

Table 7
Hourly load data for 420 units system.

1	2	3	4	5	6	7	8	9	10	11	12
105,000	112,500	118,500	123,000	127,500	130,500	133,500	141,000	144,000	147,000	148,500	150,000
13	14	15	16	17	18	19	20	21	22	23	24
144,900	136,500	130,500	127,800	126,000	129,000	135,000	138,000	144,600	128,400	120,000	108,000

points. In case of RMSE, the values are as follows for the first and second load point; 18.79 and 22.63.

Fig. 18 represents an overall comparison of NRMSE for all three studied test cases with respect to different load points. For simplicity of understanding the values are shown in descending order. As is seen, the LSSVM-CA3 has an outstanding performance in comparison to the other methods for all the different load points. The color-bar on the right-hand side of Fig. 18 represents the details of measured values.

3.4. Test case 4

To demonstrate the practicality of the proposed method for a real-time analysis on a large-scale of a realistic power system, the proposed method is investigated on the largest ever reported test system with a non-convex objective function. This test system consists of 420 generating units, which is comprised of 120 coal units, 153 LNG units, 60 nuclear units, and 87 oil units. This test

system has been made by three times replication of the 140-unit system of case 3. The considerable increase in the number of generating units, considering the physical constraints of the generators, imposes a substantial complexity into the real-time analysis of the CEED problem due to the high number of discontinuities caused by POZs, as this leads to the increased number of possible local minima.

Table 7 lists the hourly load demand of the system (all the values are expressed in MW), where the lowest load of the day and peak demand are equal to 105,000 MW and 150,000 MW, respectively. Two random load points which have been used for the prediction purposes are equal to 125,000 MW and 139,000 MW. Figs. 19 and 20 show the residuals representation of all the compared methods for both the load points. Among all the compared methods, the proposed method represents the highest accuracy for both load points. The placement of the residuals within the confidence bound for the different subsets of the two selected load points are, 89.82% for the training phase, 96.40% for

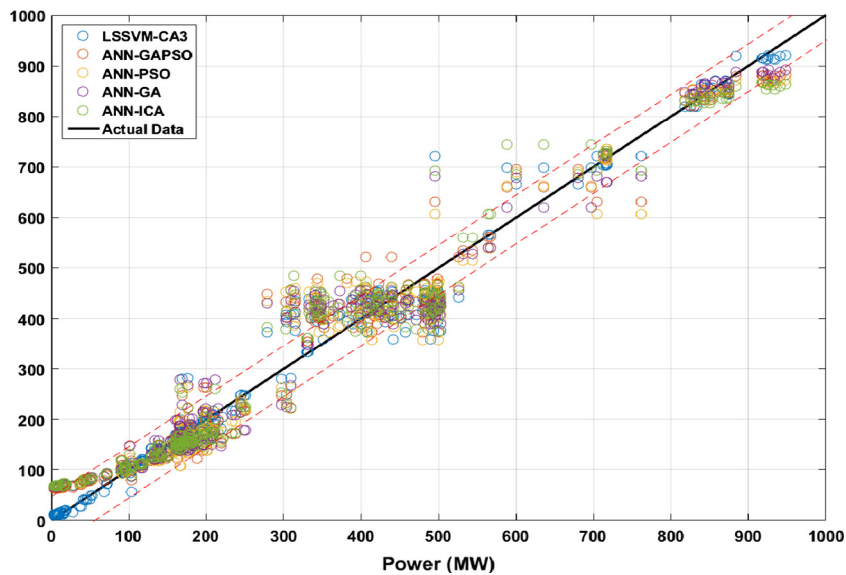


Fig. 19a. Residual representation for the first predicted load point (125,000 MW) of case 4, training phase.

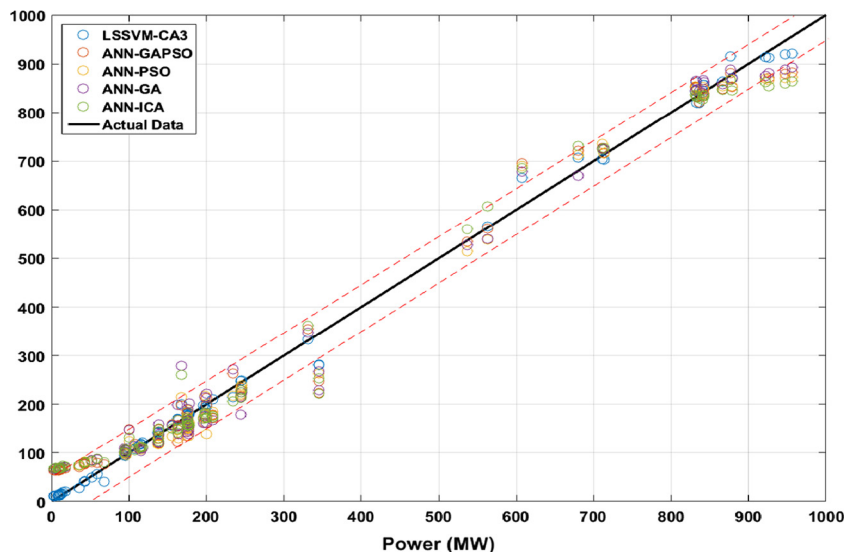


Fig. 19b. Residual representation for the first predicted load point (125,000 MW) of case 4, testing phase.

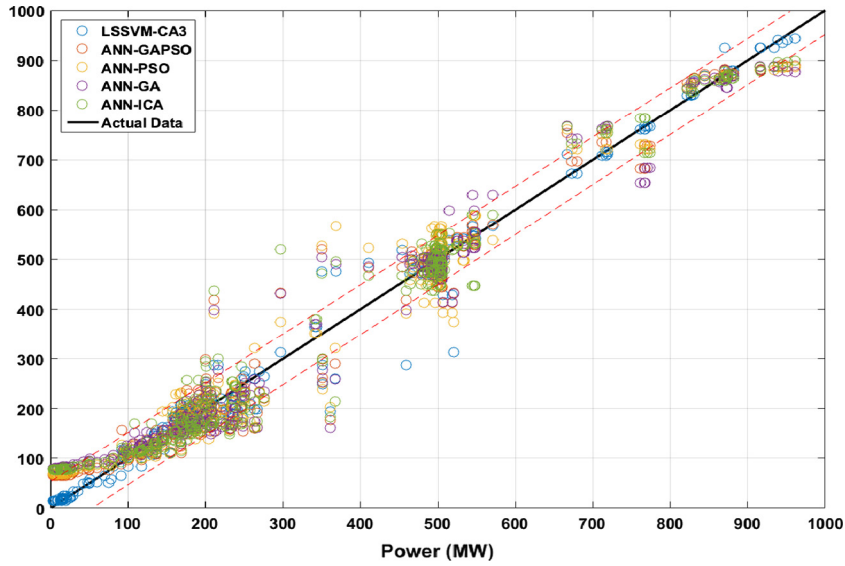


Fig. 20a. Residual representation for the second predicted load point (139,000 MW) of case 4, training phase.

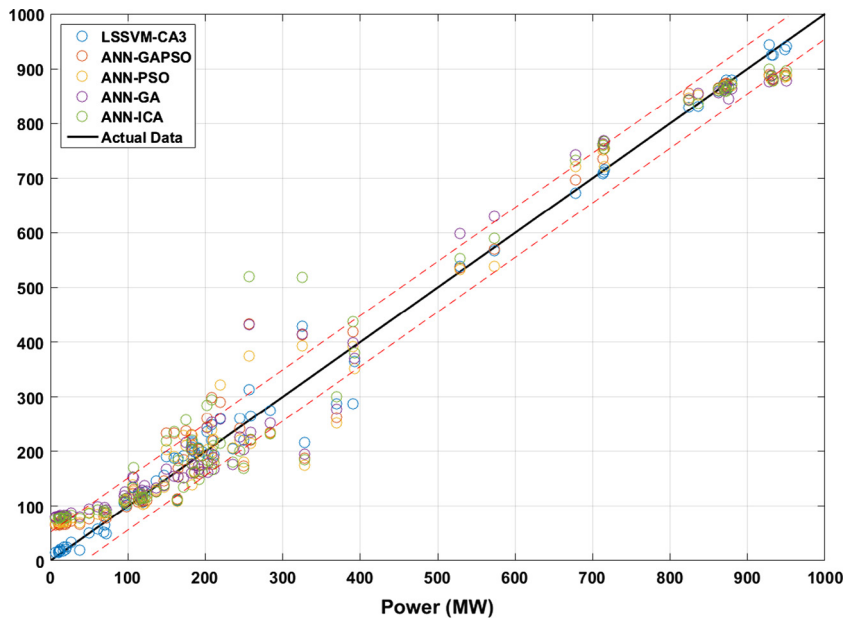


Fig. 20b. Residual representation for the second predicted load point (139,000 MW) of case 4, testing phase.

Table 8
Final optimized values for LSSVM-CA3 adjusting parameters (420 units system).

Load point (MW)	γ	σ^2
125,000	14.37	7.29
139,000	16.75	13.58

the testing phase for the first load point. In the case of the second load point, the performance of the proposed method is considerably noticeable by having 96.10% precision of prediction for the training phase and 96.40% for the testing phase.

Table 8 arranges the best-achieved values of the adjusting parameters for the LSSVM-CA3. Table 9 presents the detailed analysis of all the compared methods. From Table 9, it is obvious that the LSSVM-CA3 has acquired the lowest average and minimum total generation cost if compared to other methods in a very fast

Table 9
Comparison of the obtained results for MSE (420 units system).

	Min	Avg	Max	Avg elapsed time (s)
<i>125,000 MW</i>				
LSSVM-CA3	1127.21	1228.66	1271.39	12.24
ANN-GAPSO	1999.19	2145.31	2489.54	269.73
ANN-PSO	2036.18	2245.84	2781.65	37.21
ANN-GA	2058.44	2325.28	2844.63	38.33
ANN-ICA	2146.91	2574.25	3122.88	254.78
MIQP	945.28
<i>139,000 MW</i>				
LSSVM-CA3	860.52	918.28	960.56	12.35
ANN-GAPSO	1765.95	2001.85	2102.25	273.25
ANN-PSO	1998.77	2135.14	2345.57	38.01
ANN-GA	2075.43	2185.47	2441.43	38.55
ANN-ICA	2284.82	2236.49	2564.78	261.05
MIQP	967.48

Table 10
Comparison of the obtained results for the error analysis (420 units system).

	MAE	RMSE	NRMSE
<i>125,000 MW</i>			
LSSVM-CA3	18.69	33.57	0.1306
ANN-GAPSO	33.48	44.71	0.1739
ANN-PSO	34.25	45.12	0.1755
ANN-GA	35.22	45.37	0.1765
ANN-ICA	35.51	46.33	0.1802
<i>139,000 MW</i>			
LSSVM-CA3	17.34	29.33	0.1106
ANN-GAPSO	30.31	42.02	0.1584
ANN-PSO	33.63	44.71	0.1685
ANN-GA	33.54	45.56	0.1718
ANN-ICA	35.44	47.79	0.1831

running time considering the higher complication of the analysis for this large system. The fast convergence and evaluation of the proposed method in solving the large-scale of CEED problem indicates its capability to be used by the system operators in any real-time electricity market.

Table 11
Results of random execution of the proposed algorithm (15 units system).

15 units, LSSVM-CA3								
	1600 MW				2475 MW			
	1	2	3	4	1	2	3	4
γ	134.62	89.66	109.49	97.58	651618.64	593539.57	564871.98	581544.05
σ^2	2.59	2.47	2.80	2.61	49.85	48.29	53.17	46.37
MSE	43.47	9.13	8.05	11.86	8.20	16.89	5.53	6.98
Time (s)	0.15	0.28	0.35	0.41	0.54	0.19	0.11	0.21

Table 12
Results of random execution of the proposed algorithm (40 units system).

40 units, LSSVM-CA3								
	7550 MW				8260 MW			
	1	2	3	4	1	2	3	4
γ	24.20	23.38	27.29	29.56	76952.81	65268.83	54821.75	74512.04
σ^2	4.22	4.89	5.51	6.57	3.61	7.04	5.29	4.63
MSE	1072.31	948.55	642.44	725.00	1137.85	2868.31	1831.42	1629.26
Time (s)	1.35	2.35	1.30	1.27	2.33	2.84	1.37	1.04

Table 13
Results of random execution of the proposed algorithm (140 units system).

140 units, LSSVM-CA3								
	36,500 MW				41,800 MW			
	1	2	3	4	1	2	3	4
γ	81268.28	53283.26	48517.25	63152.58	27.28	43.50	37.91	109.82
σ^2	45257.32	29061.55	18572.36	27345.85	5.76	6.49	4.74	7.35
MSE	402.81	386.16	354.74	369.22	520.67	494.13	509.15	491.17
Time (s)	3.21	1.77	2.10	1.95	2.45	1.44	1.87	1.23

Table 14
Comparison of the proposed algorithm with the higher number of the population size of ANN-GAPSO (15 units system).

15 units								
	1600 MW				2475 MW			
	LSSVM-CA3	80	100	150	LSSVM-CA3	80	100	150
MSE	12.72	30.80	30.27	21.23	0.78	89.52	63.11	13.31
Avg elapsed time (s)	0.13	18.45	25.38	45.12	0.14	19.25	26.54	44.75

Lastly, the performance of all methods are studied by three other statistical methods; RMSE, NRMSE, and MAE, where their results have been tabulated in Table 10. From Table 10, it is very clear that the LSSVM-CA3 has obtained the lowest error among the others by a significant amount, which emphasizes the superiority of the proposed method in a real-time analysis.

3.5. Test case 5

To further clarify on the performance of the proposed method, several scenarios from the different technical point of view have been considered. For the first scenario, to demonstrate the replicability of the proposed method of the study, for each studied test case, the proposed algorithm has been randomly executed four times for each load point of the test system, where the results are tabulated in Tables 11–13.

From the acquired results in Tables 11–13, it can be seen that, all of the solutions are within the range of the presented results in the previous sections.

Table 15
Comparison of the proposed algorithm with the higher number of the population size of ANN-GAPSO (40 units system).

40 units								
	7550 MW				8260 MW			
	LSSVM-CA3	80	100	150	LSSVM-CA3	80	100	150
MSE	753.99	1569.92	1491.57	1100.91	1090.65	3088.06	2814.72	1249.17
Avg elapsed time (s)	1.55	25.32	36.45	85.37	1.29	23.61	41.25	91.54

Table 16
Comparison of the proposed algorithm with the higher number of the population size of ANN-GAPSO (140 units system).

140 units								
	36,500 MW				41,800 MW			
	LSSVM-CA3	80	100	150	LSSVM-CA3	80	100	150
MSE	353.14	383.27	374.53	373.05	512.04	1077.49	983.83	949.66
Avg elapsed time (s)	1.87	57.02	94.83	178.77	1.95	53.11	110.46	195.26

Table 17
Comparison of the proposed algorithm with LSSVM-GAPSO (15 units system).

15 units				
	1600 MW		2475 MW	
	LSSVM-CA3	LSSVM-GAPSO	LSSVM-CA3	LSSVM-GAPSO
γ	114.21	118.06	743710.44	610051.29
σ^2	3.24	3.21	68.84	108.84
MSE	12.72	12.79	0.78	12.23
Avg elapsed time (s)	0.13	0.99	0.14	1.23

Table 18
Comparison of the proposed algorithm with LSSVM-GAPSO (40 units system).

40 units				
	7550 MW		8260 MW	
	LSSVM-CA3	LSSVM-GAPSO	LSSVM-CA3	LSSVM-GAPSO
γ	26.88	29.19	74390.99	65450.24
σ^2	7.4	8.01	5.99	11.79
MSE	753.99	1077.79	1090.65	1174.67
Avg elapsed time (s)	1.55	2.73	1.29	7.84

Table 19
Comparison of the proposed algorithm with LSSVM-GAPSO (140 units system).

140 units				
	36,500 MW		41,800 MW	
	LSSVM-CA3	LSSVM-GAPSO	LSSVM-CA3	LSSVM-GAPSO
γ	63381.17	59346.85	23.56	307.87
σ^2	26822.02	24136.10	4.71	18.95
MSE	353.14	365.57	512.04	721.53
Avg elapsed time (s)	1.87	2.47	1.95	3.41

For the second scenario, due to different characteristics of the optimization algorithms, the best population size, and parameters of various optimization methods could be different. As ANN-GAPSO has shown the best performance among all the other ANN based methods according to the results in the previous test cases, the population size of GAPSO has been adjusted to obtain its best performance. Therefore, to investigate the ability of ANN-

GAPSO with a higher number of swarms or agents in the search space, its population size has been increased to 80,100 and 150, while its results have been compared to LSSVM-CA3 (for comparable results, ANN-GAPSO has been performed 20 times). The results of this scenario are presented in Tables 14–16.

As it can be seen from the results, by increasing the population size of the GAPSO, the total performance of ANN-GAPSO has been considerably improved, however, due to the increment in population size of GAPSO, the total running time of the ANN-GAPSO has also been significantly increased, which does not make the approach suitable for real-time analysis. Whereas, the proposed method has achieved a better solution in a lower time.

For the third scenario, to demonstrate the advantage of LSSVM-CA3 in comparison to the combination of the other algorithms with LSSVM, the GAPSO has been combined with LSSVM (GAPSO has been selected to be compared with LSSVM for the same reason as the previous scenario). To have comparable results, the population sizes of both optimizers were set to 50 and have been executed 20 times. The results are charted in Tables 17–19.

From Tables 17–19, it is evident that the proposed method (LSSVM-CA3) outperforms LSSVM-GAPSO with a considerable difference in all the studied cases.

4. Conclusions

An accurate, fast and reliable method of dispatching generating resources is a critical tool in the real-time electricity market to ensure the delivery of consistent and economic electricity services to all the grid-connected customers. In this paper, a hybrid mathematical model based on LSSVM and CA3 for optimal scheduling of generating units in the context of a real-time electricity market has been proposed. Several physical constraints and environmental impacts of the generating units through different test systems were considered and analyzed to demonstrate the practicality and efficiency of the proposed model. The optimal scheduling for the hourly load curve of the test systems has been prepared by the MIQP for training purposes. The comparison cases were performed between LSSVM-CA3 and other ANN coupled prediction methods. According to the obtained results of the proposed method the following conclusions can be drawn:

- The proposed model demonstrated superior stable performance in optimal scheduling of the generating units and achieved the lowest values of MSE, RMSE, and MAE compared to other hybrid well-established ANN methods which are widely used for power market forecasting.

Table A.1
15 units system characteristics.

Unit no.	P_i^{min} (MW)	P_i^{max} (MW)	a_i (\$/h)	b_i (\$/MW h)	c_i (\$/MW ² h)	P_i^0 (MW)	UR_i (MW)	DR_i (MW)
1	150	455	671	10.1	0.000299	400	80	120
2	150	455	574	10.2	0.000183	300	80	120
3	20	130	374	8.8	0.001126	105	130	130
4	20	130	374	8.8	0.001126	100	130	130
5	150	470	461	10.4	0.000205	90	80	120
6	135	460	630	10.1	0.000301	400	80	120
7	135	465	548	9.8	0.000364	350	80	120
8	60	300	227	11.2	0.000338	95	65	100
9	25	162	173	11.2	0.000807	105	60	100
10	25	160	175	10.7	0.001203	110	60	100
11	20	80	186	10.2	0.003586	60	80	80
12	20	80	230	9.9	0.005513	40	80	80
13	25	85	225	13.1	0.000371	30	80	80
14	15	55	309	12.1	0.001929	20	55	55
15	15	55	323	12.4	0.004447	20	55	55

- The proposed method acquired the lowest residual values with the highest placement of the predictions within the confidence bound in a very fast processing time in comparison to all other methods of ANN, and where the reduction percentage in processing time compared to MIQP is almost equal to 99% for the first and the third test case and 60% for the second test case.
- Analysis of the NRMSE shows the excellent performance of LSSVM-CA3 compared to other methods for all the studied cases.
- The proposed method is capable of understanding the equality and inequality constraints of generating units as well as adhering to their physical and environmental constraints.
- The proposed method has adopted a tuning optimizer for its adjusting parameters (γ and σ^2) to obtain the best possible solution without the interference of the human experience during the optimization process.

According to all above mentioned facts and the considerable accuracy of the obtained results, it implies that the proposed model of the study is applicable to the real-time power market.

Appendix A

For ease of reference all the system specifications which have been used in the studied cases is given in this section. In this appendix all the required data for the 15 units system is given (all the units are thermal). This data is based in [58]. Unit data can be found in Tables A.1 and A.2.

Appendix B

In this appendix all the required data for the 40 units system is given (all the units are thermal). This data is based in [45]. Unit data is given in Table B.1.

Appendix C

In this appendix all the required data for the 140 units system is given. This data is based in [59]. Unit data can be found in Tables C.1–C.3.

Table A.2
Prohibited operating zones of 15 units system.

Unit no.	Prohibited operating zones (MW)
2	[185 225][305 335][420 450]
5	[180 200][305 335][390 420]
6	[230 255][365 395][430 455]
12	[30 40][55 65]

Table B.1
40 units system characteristics.

Unit no.	P_i^{min} (MW)	P_i^{max} (MW)	a_i (\$/h)	b_i (\$/ MW h)	c_i (\$/ MW ² h)	d_i (\$/h)	e_i (rad/ MW)	α_i (ton/h)	β_i (ton/ MW h)	γ_i (ton/ MW ² h)	η_i (ton/h)	δ_i (1/MW)
1	36	114	94.705	6.73	0.0069	100	0.084	60	-2.22	0.048	1.31	0.0569
2	36	114	94.705	6.73	0.0069	100	0.084	60	-2.22	0.048	1.31	0.0569
3	60	120	309.54	7.07	0.02028	100	0.084	100	-2.36	0.0762	1.31	0.0569
4	80	190	369.03	8.18	0.00942	150	0.063	120	-3.14	0.054	0.9142	0.0454
5	47	97	148.89	5.35	0.0114	120	0.077	50	-1.89	0.085	0.9936	0.0406
6	68	140	222.33	8.05	0.01142	100	0.084	80	-3.08	0.0854	1.31	0.0569
7	110	300	287.71	8.03	0.00357	200	0.042	100	-3.06	0.0242	0.655	0.02846
8	135	300	391.98	6.99	0.00492	200	0.042	130	-2.32	0.031	0.655	0.02846
9	135	300	455.76	6.6	0.00573	200	0.042	150	-2.11	0.0335	0.655	0.02846
10	130	300	722.82	12.9	0.00605	200	0.042	280	-4.34	0.425	0.655	0.02846
11	94	375	635.2	12.9	0.00515	200	0.042	220	-4.34	0.0322	0.655	0.02846
12	94	375	654.69	12.8	0.00569	200	0.042	225	-4.28	0.0338	0.655	0.02846
13	125	500	913.4	12.5	0.00421	300	0.035	300	-4.18	0.0296	0.5035	0.02075
14	125	500	1760.4	8.84	0.00752	300	0.035	520	-3.34	0.0512	0.5035	0.02075
15	125	500	1760.4	8.84	0.00752	300	0.035	510	-3.55	0.0496	0.5035	0.02075
16	125	500	1760.4	8.84	0.00752	300	0.035	510	-3.55	0.0496	0.5035	0.02075
17	220	500	647.85	7.97	0.00313	300	0.035	220	-2.68	0.0151	0.5035	0.02075
18	220	500	649.69	7.95	0.00313	300	0.035	222	-2.66	0.0151	0.5035	0.02075

Table B.1 (continued)

Unit no.	P_i^{min} (MW)	P_i^{max} (MW)	a_i (\$/h)	b_i (\$/MW h)	c_i (\$/MW ² h)	d_i (\$/h)	e_i (rad/MW)	α_i (ton/h)	β_i (ton/MW h)	γ_i (ton/MW ² h)	η_i (ton/h)	δ_i (1/MW)
19	242	550	647.83	7.97	0.00313	300	0.035	220	-2.68	0.0151	0.5035	0.02075
20	242	550	647.81	7.97	0.00313	300	0.035	220	-2.68	0.0151	0.5035	0.02075
21	254	550	785.96	6.63	0.00298	300	0.035	290	-2.22	0.0145	0.5035	0.02075
22	254	550	785.96	6.63	0.00298	300	0.035	285	-2.22	0.0145	0.5035	0.02075
23	254	550	794.53	6.66	0.00284	300	0.035	295	-2.26	0.0138	0.5035	0.02075
24	254	550	794.53	6.66	0.00284	300	0.035	295	-2.26	0.0138	0.5035	0.02075
25	254	550	801.32	7.1	0.00277	300	0.035	310	-2.42	0.0132	0.5035	0.02075
26	254	550	801.32	7.1	0.00277	300	0.035	310	-2.42	0.0132	0.5035	0.02075
27	10	150	1055.1	3.33	0.52124	120	0.077	360	-1.11	1.842	0.9936	0.0406
28	10	150	1055.1	3.33	0.52124	120	0.077	360	-1.11	1.842	0.9936	0.0406
29	10	150	1055.1	3.33	0.52124	120	0.077	360	-1.11	1.842	0.9936	0.0406
30	47	97	148.89	5.35	0.0114	120	0.077	50	-1.89	0.085	0.9936	0.0406
31	60	190	222.92	6.43	0.0016	150	0.063	80	-2.08	0.0121	0.9142	0.0454
32	60	190	222.92	6.43	0.0016	150	0.063	80	-2.08	0.0121	0.9142	0.0454
33	60	190	222.92	6.43	0.0016	150	0.063	80	-2.08	0.0121	0.9142	0.0454
34	90	200	107.87	8.95	0.0001	200	0.042	65	-3.48	0.0012	0.655	0.02846
35	90	200	116.58	8.62	0.0001	200	0.042	70	-3.24	0.0012	0.655	0.02846
36	90	200	116.58	8.62	0.0001	200	0.042	70	-3.24	0.0012	0.655	0.02846
37	25	110	307.45	5.88	0.0161	80	0.098	100	-1.98	0.095	1.42	0.0677
38	25	110	307.45	5.88	0.0161	80	0.098	100	-1.98	0.095	1.42	0.0677
39	25	110	307.45	5.88	0.0161	80	0.098	100	-1.98	0.095	1.42	0.0677
40	242	550	647.83	7.97	0.00313	300	0.035	220	-2.68	0.0151	0.5035	0.02075

Table C.1
140 units system characteristics.

Unit no.	P_i^{min} (MW)	P_i^{max} (MW)	a_i (\$/h)	b_i (\$/MW h)	c_i (\$/MW ² h)	P_i^0 (MW)	UR_i (MW)	DR_i (MW)
Coal#01	71	119	1220.645	61.242	0.032888	98.4	30	120
Coal#02	120	189	1315.118	41.095	0.00828	134	30	120
Coal#03	125	190	874.288	46.31	0.003849	141.5	60	60
Coal#04	125	190	874.288	46.31	0.003849	183.33	60	60
Coal#05	90	190	1976.469	54.242	0.042468	125	150	150
Coal#06	90	190	1338.087	61.215	0.014992	91.3	150	150
Coal#07	280	490	1818.299	11.791	0.007039	401.1	180	300
Coal#08	280	490	1133.978	15.055	0.003079	329.5	180	300
Coal#09	260	496	1320.636	13.226	0.005063	356.1	300	510
Coal#10	260	496	1320.636	13.226	0.005063	427.3	300	510
Coal#11	260	496	1320.636	13.226	0.005063	412.2	300	510
Coal#12	260	496	1106.539	14.498	0.003552	370.1	300	510
Coal#13	260	506	1176.504	14.651	0.003901	301.8	600	600
Coal#14	260	509	1176.504	14.651	0.003901	368	600	600
Coal#15	260	506	1176.504	14.651	0.003901	301.9	600	600
Coal#16	260	505	1176.504	14.651	0.003901	476.4	600	600
Coal#17	260	506	1017.406	15.669	0.002393	283.1	600	600
Coal#18	260	506	1017.406	15.669	0.002393	414.1	600	600
Coal#19	260	505	1229.131	14.656	0.003684	328	600	600
Coal#20	260	505	1229.131	14.656	0.003684	389.4	600	600
Coal#21	260	505	1229.131	14.656	0.003684	354.7	600	600
Coal#22	260	505	1229.131	14.656	0.003684	262	600	600
Coal#23	260	505	1267.894	14.378	0.004004	461.5	600	600
Coal#24	260	505	1229.131	14.656	0.003684	371.6	600	600
Coal#25	280	537	975.926	16.261	0.001619	462.6	300	300
Coal#26	280	537	1532.093	13.362	0.005093	379.2	300	300
Coal#27	280	549	641.989	17.203	0.000993	530.8	360	360
Coal#28	280	549	641.989	17.203	0.000993	391.9	360	360
Coal#29	260	501	911.533	15.274	0.002473	480.1	180	180
Coal#30	260	501	910533	15.212	0.002547	319	180	180
Coal#31	260	506	1074.81	15.033	0.003542	329.5	600	600
Coal#32	260	506	1074.81	15.033	0.003542	333.8	600	600
Coal#33	260	506	1074.81	15.033	0.003542	390	600	600
Coal#34	260	506	1074.81	15.033	0.003542	432	600	600
Coal#35	260	500	1278.46	13.992	0.003132	402	660	660
Coal#36	260	500	861.742	15.679	0.001323	428	900	900
Coal#37	120	241	408.834	16.542	0.00295	178.4	180	180
Coal#38	120	241	408.834	16.542	0.00295	194.1	180	180
Coal#39	423	774	1288.815	16.518	0.000991	474	600	600
Coal#40	423	769	1436.251	15.815	0.001581	609.8	600	600
LNG#1	3	19	669.988	75.464	0.90236	17.8	210	210
LNG#2	3	28	134.544	129.544	0.110295	6.9	366	366
LNG-CC#1	160	250	3427.912	56.613	0.024493	224.3	702	702
LNG-CC#2	160	250	3751.722	54.451	0.029156	210	702	702

(continued on next page)

Table C.1 (continued)

Unit no.	P_i^{\min} (MW)	P_i^{\max} (MW)	a_i (\$/h)	b_i (\$/MW h)	c_i (\$/MW ² h)	P_i^0 (MW)	UR_i (MW)	DR_i (MW)
LNG-CC#3	160	250	3918.78	54.736	0.024667	212	702	702
LNG-CC#4	160	250	3379.58	58.034	0.016517	200.8	702	702
LNG-CC#5	160	250	3345.296	55.981	0.026584	220	702	702
LNG-CC#6	160	250	3138.754	61.52	0.00754	232.9	702	702
LNG-CC#7	160	250	3453.05	58.635	0.01643	168	702	702
LNG-CC#8	160	250	5119.3	44.647	0.045934	208.4	702	702
LNG-CC#9	165	504	1898.415	71.584	0.000044	443.9	1350	1350
LNG-CC#10	165	504	1898.415	71.584	0.000044	426	1350	1350
LNG-CC#11	165	504	1898.415	71.584	0.000044	434.1	1350	1350
LNG-CC#12	165	504	1898.415	71.584	0.000044	402.5	1350	1350
LNG-CC#13	180	471	2473.39	85.12	0.002528	357.4	1350	1350
LNG-CC#14	180	561	2781.705	87.682	0.000131	423	720	720
LNG-CC#15	103	341	5515.508	69.532	0.010372	220	720	720
LNG-CC#16	100	312	6240.909	58.172	0.012464	273.5	1500	1500
LNG-CC#17	153	471	9960.11	46.636	0.039441	336	1656	1656
LNG-CC#18	163	500	3671.977	76.947	0.007278	432	2160	2160
LNG-CC#19	95	302	1837.383	80.761	0.000044	220	900	900
LNG-CC#20	160	511	3108.395	70.136	0.000044	410.6	1200	1200
LNG-CC#21	160	511	3108.395	70.136	0.000044	422.7	1200	1200
LNG-CC#22	196	490	7095.484	49.84	0.018827	351	1014	1014
LNG-CC#23	196	490	3392.732	65.404	0.010852	296	1014	1014
LNG-CC#24	196	490	7095.484	49.84	0.018827	411.1	1014	1014
LNG-CC#25	196	490	7095.484	49.84	0.018827	263.2	1014	1014
LNG-CC#26	130	432	4288.32	66.645	0.03456	370.3	1350	1350
LNG-CC#27	130	432	13813.001	22.941	0.08154	418.7	1350	1350
LNG-CC#28	137	455	4435.493	64.314	0.023534	409.6	1350	1350
LNG-CC#29	137	455	9750.75	45.017	0.035475	412	1350	1350
LNG-CC#30	195	541	1042.366	70.644	0.000915	423.2	780	780
LNG-CC#31	175	536	1159.895	70.959	0.000044	428	1650	1650
LNG-CC#32	175	540	1159.895	70.959	0.000044	436	1650	1650
LNG-CC#33	175	538	1303.99	70.302	0.001307	428	1650	1650
LNG-CC#34	175	540	1156.193	70.662	0.000392	425	1650	1650
LNG-CC#35	330	574	2118.968	71.101	0.000087	497.2	1620	1620
LNG-CC#36	160	531	779.519	37.854	0.000521	510	1482	1482
LNG-CC#37	160	531	829.888	37.768	0.000498	470	1482	1482
LNG-CC#38	200	542	2333.69	67.983	0.001046	464.1	1668	1668
LNG-CC#39	56	132	2028.954	77.838	0.13205	118.1	120	120
LNG-CC#40	115	245	4412.017	63.671	0.096968	141.3	180	180
LNG-CC#41	115	245	2982.219	79.458	0.054868	132	120	180
LNG-CC#42	115	245	2982.219	79.458	0.054868	135	120	180
LNG-CC#43	207	307	3174.939	93.966	0.014382	252	120	180
LNG-CC#44	207	307	3218.359	94.723	0.013161	221	120	180
LNG-CC#45	175	345	3723.822	66.919	0.016033	245.9	318	318
LNG-CC#46	160	531	779.519	37.854	0.000521	510	1482	1482
LNG-CC#47	175	345	3551.405	68.185	0.013653	247.9	318	318
LNG-CC#48	175	345	4322.165	60.821	0.028148	183.6	318	318
LNG-CC#49	175	345	3493.739	68.551	0.01347	288	318	318
NUCLEAR#01	360	580	226.799	2.842	0.000064	557.4	18	18
NUCLEAR#02	415	645	382.932	2.946	0.000252	529.5	18	18
NUCLEAR#03	795	984	156.987	3.096	0.000022	800.8	36	36
NUCLEAR#04	795	978	154.484	3.04	0.000022	801.5	36	36
NUCLEAR#05	578	682	332.834	1.709	0.000203	582.7	138	204
NUCLEAR#06	615	720	326.599	1.668	0.000198	680.7	144	216
NUCLEAR#07	612	718	345.306	1.789	0.000215	670.7	144	216
NUCLEAR#08	612	720	350.372	1.815	0.000218	651.7	144	216
NUCLEAR#09	758	964	370.377	2.726	0.000193	921	48	48
NUCLEAR#10	755	958	367.067	2.732	0.000197	916.8	48	48
NUCLEAR#11	750	1007	124.875	2.651	0.000324	911.9	36	54
NUCLEAR#12	750	1006	130.785	2.798	0.000344	898	36	54
NUCLEAR#13	713	1013	878.746	1.595	0.00069	905	30	30
NUCLEAR#14	718	1020	827.959	1.503	0.00065	846.5	30	30
NUCLEAR#15	791	954	432.007	2.425	0.000233	850.9	30	30
NUCLEAR#16	786	952	445.606	2.499	0.000239	843.7	30	30
NUCLEAR#17	795	1006	467.223	2.674	0.000261	841.4	36	36
NUCLEAR#18	795	1013	475.94	2.692	0.000259	835.7	36	36
NUCLEAR#19	795	1021	899.462	1.633	0.000707	828.8	36	36
NUCLEAR#20	795	1015	1000.367	1.816	0.000786	846	36	36
OIL#01	94	203	1269.132	98.83	0.014355	179	120	120
OIL#02	94	203	1269.132	89.83	0.014355	120.8	120	120
OIL#03	94	203	1269.132	89.83	0.014355	121	120	120
OIL#04	244	379	4965.124	64.125	0.030266	317.4	480	480
OIL#05	244	379	4965.124	64.125	0.030266	318.4	480	480
OIL#06	244	379	4965.124	64.125	0.030266	335.8	480	480
OIL#07	95	190	2243.185	76.129	0.024027	151	240	240
OIL#08	95	189	2290.381	81.805	0.00158	129.5	240	240

Table C.1 (continued)

Unit no.	P_i^{min} (MW)	P_i^{max} (MW)	a_i (\$/h)	b_i (\$/MW h)	c_i (\$/MW ² h)	P_i^0 (MW)	UR_i (MW)	DR_i (MW)
OIL#09	116	194	1681.533	81.14	0.022095	130	120	120
OIL#10	175	321	6743.302	46.665	0.07681	218.9	180	180
OIL#11	2	19	394.398	78.412	0.953443	5.4	90	90
OIL#12	4	59	1243.165	112.088	0.000044	45	90	90
OIL#13	15	83	1454.74	90.871	0.072468	20	300	300
OIL#14	9	53	1011.051	97.116	0.000448	16.3	162	162
OIL#15	12	37	909.269	83.244	0.599112	20	114	114
OIL#16	10	34	689.378	95.665	0.244706	22.1	120	120
OIL#17	112	373	1443.792	91.202	0.000042	125	1080	1080
OIL#18	4	20	535.553	104.501	0.085145	10	60	60
OIL#19	5	38	617.734	83.015	0.524718	13	66	66
OIL#20	5	19	90.966	127.795	0.176515	7.5	12	6
OIL#21	50	98	974.447	77.929	0.063414	53.2	300	300
OIL#22	5	10	263.81	92.779	2.740485	6.4	6	6
OIL#23	42	74	1335.594	80.95	0.112438	69.1	60	60
OIL#24	42	74	1033.871	89.073	0.041529	49.9	60	60
OIL#25	41	105	1391.325	161.288	0.000911	91	528	528
OIL#26	17	51	4477.11	161.829	0.005245	41	300	300
OIL#27	7	19	57.794	84.972	0.234787	13.7	18	30
OIL#28	7	19	57.794	84.972	0.234787	7.4	18	30
OIL#29	26	40	1258.437	16.087	1.111878	28.6	72	120

Table C.2

Valve-point data of 140 units system with unit characteristics.

Unit no.	a_i (\$/h)	b_i (\$/MW h)	c_i (\$/MW ² h)	d_i (\$/h)	e_i (rad/MW)
COAL#05	1976.469	54.242	0.042468	700	0.080
COAL#10	1320.636	13.226	0.005063	600	0.055
COAL#15	1176.504	14.651	0.003901	800	0.060
COAL#22	1229.131	14.656	0.003684	600	0.050
COAL#33	1074.810	15.033	0.003542	600	0.043
COAL#40	1436.251	15.815	0.001581	600	0.043
LNG_CC#10	1898.415	71.584	0.000044	1100	0.043
LNG_CC#28	13813.001	22.941	0.081540	1200	0.030
LNG_CC#30	9750.750	45.017	0.035475	1000	0.050
LNG_CC#42	2982.219	79.458	0.054868	1000	0.050
OIL#08	2290.381	81.805	0.001580	600	0.070
OIL#10	6743.302	46.665	0.076810	1200	0.043

Table C.3

Prohibited operating zones of 140 units system.

Unit no.	Prohibited operating zones (MW)
COAL#08	[250 280][305 335][420 450]
COAL#32	[220 250][320 350][390 420]
LNG_CC#32	[230 255][365 395][430 455]
OIL#25	[50 75][85 95]

References

[1] Vagropoulos SI, Kardakos EG, Simoglou CK, Bakirtzis AG, Catalao JPS. ANN-based scenario generation methodology for stochastic variables of electric power systems. *Electric Power Syst Res* 2016;134:9–18.

[2] (EU) EC. *Energy roadmap*, 2050; 2012.

[3] Dieu VN, Schegner P. Augmented Lagrange Hopfield network initialized by quadratic programming for economic dispatch with piecewise quadratic cost functions and prohibited zones. *Appl Soft Comput* 2013;13:292–301.

[4] Mousa AAA. Hybrid ant optimization system for multiobjective economic emission load dispatch problem under fuzziness. *Swarm Evol Comput* 2014;18:11–21.

[5] Afzalan E, Joorabian M. An improved cuckoo search algorithm for power economic load dispatch. *Int Trans Electr Energy* 2015;25:958–75.

[6] Koltsaklis NE, Georgiadis MC. A multi-period, multi-regional generation expansion planning model incorporating unit commitment constraints. *Appl Energy* 2015;158:310–31.

[7] Koltsaklis NE, Dagoumas AS, Georgiadis MC, Papaioannou G, Dikaiakos C. A midterm, market-based power systems planning model. *Appl Energy* 2016;179:17–35.

[8] Niknam T, Khodaei A, Fallahi F. A new decomposition approach for the thermal unit commitment problem. *Appl Energy* 2009;86:1667–74.

[9] Simoglou CK, Biskas PN, Bakirtzis AG. Optimal self-scheduling of a thermal producer in short-term electricity markets by MILP. *IEEE Trans Power Syst* 2010;25(4):1965–77.

[10] Delarue E, D'haeseleer W. Adaptive mixed-integer programming unit commitment strategy for determining the value of forecasting. *Appl Energy* 2008;85:171–81.

[11] Lima RM, Novais AQ. Symmetry breaking in MILP formulations for unit commitment problems. *Comput Chem Eng* 2016;85:162–76.

[12] Wang J, Botterud A, Bessa R, Keko H, Carvalho L, Issicaba D, et al. Wind power forecasting uncertainty and unit commitment. *Appl Energy* 2011;88:4014–23.

[13] Wang J, Wang J, Liu C, Ruiz JP. Stochastic unit commitment with sub-hourly dispatch constraints. *Appl Energy* 2013;105:418–22.

[14] Baskar S, Subbaraj P, Rao MVC. Hybrid real coded genetic algorithm solution to economic dispatch problem. *Comput Electr Eng* 2003;29:407–19.

[15] Mohammadi-ivatloo B, Rabiee A, Ehsan M. Time-varying acceleration coefficients IPSO for solving dynamic economic dispatch with non-smooth cost function. *Energy Convers Manage* 2012;56:175–83.

[16] Secui DC. A new modified artificial bee colony algorithm for the economic dispatch problem. *Energy Convers Manage* 2015;89:43–62.

[17] Khorram E, Jaberipour M. Harmony search algorithm for solving combined heat and power economic dispatch problems. *Energy Convers Manage* 2011;52:1550–4.

[18] Khamasawang S, Jirivibhakorn S. DPSO-TSA for economic dispatch problem with nonsmooth and noncontinuous cost functions. *Energy Convers Manage* 2010;51:365–75.

[19] Secui DC. A method based on the ant colony optimization algorithm for dynamic economic dispatch with valve-point effects. *Int Trans Electr Energy* 2015;25:262–87.

[20] Rajagopalan A, Sengoden V, Govindasamy R. Solving economic load dispatch problems using chaotic self-adaptive differential harmony search algorithm. *Int Trans Electr Energy* 2015;25:845–58.

[21] Xiong G, Shi D, Duan X. Multi-strategy ensemble biogeography-based optimization for economic dispatch problems. *Appl Energy* 2013;111:801–11.

[22] Alsumait JS, Sykulski JK, Al-Othman AK. A hybrid GA-PS-SQP method to solve valve-point economic dispatch problems. *Appl Energy* 2010;87:1773–81.

- [23] Tsai MT, Yen CW. The influence of carbon dioxide trading scheme on economic dispatch of generators. *Appl Energy* 2011; 88: 4811–6.
- [24] Wei W, Liu F, Wang J, Chen L, Mei S, Yuan T. Robust environmental-economic dispatch incorporating wind power generation and carbon capture plants. *Appl Energy* 2016;183:674–84.
- [25] Niknam T. A new fuzzy adaptive hybrid particle swarm optimization algorithm for non-linear, non-smooth and non-convex economic dispatch problem. *Appl Energy* 2010;87:327–39.
- [26] Roy PK, Bhui S. A multi-objective hybrid evolutionary algorithm for dynamic economic emission load dispatch. *Int Trans Electr Energy* 2016;26:49–78.
- [27] Mandala M, Gupta CP. Combined economic emission dispatch based transmission congestion management under deregulated electricity market. In: International conference on computing, electronics and electrical technologies. Kumaracoil: IEEE; 2012. p. 122–7.
- [28] Vo DN, Ongsakul W. Economic dispatch with multiple fuel types by enhanced augmented Lagrange Hopfield network. *Appl Energy* 2012;91:281–9.
- [29] Canizes B, Soares J, Faria P, Vale Z. Mixed integer non-linear programming and Artificial Neural Network based approach to ancillary services dispatch in competitive electricity markets. *Appl Energy* 2013;108:261–70.
- [30] Momoh JA, Reddy SS. Combined economic and emission dispatch using radial basis function. In: IEEE PES general meeting. National Harbor, MD: IEEE; 2014. p. 1–5.
- [31] Huang CM, Wang FL. An RBF network with OLS and EPSO algorithms for real-time power dispatch. *IEEE Trans Power Syst* 2007;22:96–104.
- [32] Kar B, Mandal KK, Pal D, Chakraborty N. Combined economic and emission dispatch by ANN with backprop algorithm using variant learning rate & momentum coefficient. In: International power engineering conference. Singapore: IEEE; 2005. p. 230–5.
- [33] Lin WM, Tu CS, Yang RF, Tsai MT. Particle swarm optimisation aided least-square support vector machine for load forecast with spikes. *IET Gener Transm Dis* 2016;10:1145–53.
- [34] dos Santos GS, Luvizotto LGJ, Mariani VC, Coelho LD. Least squares support vector machines with tuning based on chaotic differential evolution approach applied to the identification of a thermal process. *Expert Syst Appl* 2012;39:4805–12.
- [35] Nagi Jea. Detection of abnormalities and electricity theft using genetic support vector machines. In: TENCON – IEEE region 10 conference. Hyderabad: IEEE; 2008. p. 1–6.
- [36] Mustafa Z, Yusof Y, Kamaruddin SS. Application of LSSVM by ABC in energy commodity price forecasting. In: IEEE 8th international power engineering and optimization conference, Langkawi; 2014. p. 94–8.
- [37] Zhang J, Lin Y, Lu P. Short-term electricity load forecasting based on ICA and LSSVM. In: International conference on computational intelligence and software engineering, Wuhan; 2009. p. 1–4.
- [38] Goudarzi A, Ahmadi A, Swanson GA, Van Coller J. Non-convex optimisation of combined environmental economic dispatch through cultural algorithm with the consideration of the physical constraints of generating units and price penalty factors. *Afr Res J, SAIEE* 2016;107:146–66.
- [39] Limited ES. Capacity market; 2016.
- [40] Shabanzadeh M. Business processes in wholesale market operation; 2016.
- [41] Catalão JPS. Smart and sustainable power systems: operations, planning, and economics of insular electricity grids. Taylor and Francis Group.
- [42] Kazemi M, Siano P, Sarno D, Goudarzi A. Evaluating the impact of sub-hourly unit commitment method on spinning reserve in presence of intermittent generators. *J Energy* 2016;113:338–54.
- [43] Decker GL, Brooks AD. Valve point loading of turbines. *Electr Eng* 2013;77:50.
- [44] Ciornei I, Kyriakides E. Recent methodologies and approaches for the economic dispatch of generation in power systems. *Int Trans Electr Energy* 2013;23:1002–27.
- [45] Guvenc U, Sonmez Y, Duman S, Yorukeren N. Combined economic and emission dispatch solution using gravitational search algorithm. *Sci Iran* 2012;19:1754–62.
- [46] Jadoun VK, Gupta N, Niazi KR, Swarnkar A. Dynamically controlled particle swarm optimization for large-scale nonconvex economic dispatch problems. *Int Trans Electr Energy* 2015;25:3060–74.
- [47] Wang SK, Chiou JP, Liu CW. Non-smooth/non-convex economic dispatch by a novel hybrid differential evolution algorithm. *IET Gener Transm Dis* 2007;1:793–803.
- [48] Zhang HF, Zhou JZ, Fang N, Zhang R, Zhang YC. Daily hydrothermal scheduling with economic emission using simulated annealing technique based multi-objective cultural differential evolution approach. *Energy* 2013;50:24–37.
- [49] Bhattacharya B, Mandal D, Chakraborty N. A multi-objective optimization based on cultural algorithm for economic dispatch with environmental constraints. *Int J Sci Eng Res* 2012;3:1–8.
- [50] Suykens JAK, Vandewalle J. Least squares support vector machine classifiers. *Neural Process Lett* 1999;9:293–300.
- [51] Suykens JAK, De Brabanter J, Lukas L, Vandewalle J. Weighted least squares support vector machines: robustness and sparse approximation. *Neurocomputing* 2002;48:85–105.
- [52] Suykens JAK. Least squares support vector machines. World Scientific Publishing Company; 2002.
- [53] Tapia R. Practical methods of optimization, Vol 2, constrained optimization – Fletcher, R. *Siam Rev* 1984;26:143–4.
- [54] Goudarzi A, Davidson IE, Ahmadi A, Venayagamoorthy GK. Intelligent analysis of wind turbine power curve. In: IEEE symposium series on computational intelligence, Orlando, Florida; 2014. p. 1–7.
- [55] Grigoriu M. Stochastic calculus: applications in science and engineering. Boston: Birkhäuser; 2002.
- [56] Novak J, Chalupa P. Implementation of mixed-integer programming on embedded system. In: 25th DAAAM international symposium on intelligent manufacturing and automation, Daaam; 2015. p. 1649–56.
- [57] Niknam T, Azizpanah-Abarghoee R, Aghaei J. A new modified teaching-learning algorithm for reserve constrained dynamic economic dispatch. *IEEE Trans Power Syst* 2013;28:749–63.
- [58] Gaing ZL. Particle swarm optimization to solving the economic dispatch considering the generator constraints. *IEEE Trans Power Syst* 2003;18:1187–95.
- [59] Park JB, Jeong YW, Shin JR, Lee KY. An improved particle swarm optimization for nonconvex economic dispatch problems. *IEEE Trans Power Syst* 2010;25:156–66.